Climatology of aerosols over the Caribbean islands: aerosol types, synoptic patterns and transport

Albeht Rodríguez Vega[1], Juan Carlos Antuña-Marrero[2],
David Barriopedro[3], Ricardo García-Herrera[3,4], Victoria E. Cachorro Revilla[2], Ángel de Frutos Baraja[2], and Juan Carlos Antuña-Sánchez[2]

[1]Atmospheric Optics Group, Meteorological Institute of Cuba, Camagüey, Cuba

[2]Group of Atmospheric Optics (GOA-UVa), Universidad de Valladolid, 47011, Valladolid, Spain

[3]Instituto de Geociencias, IGEO (CSIC-UCM), Madrid, Spain

[4]Departamento de Física de la Tierra y Astrofísica, Facultad de Ciencias Físicas, Universidad Complutense de Madrid, Madrid, Spain

Resubmitted to *Journal of Applied Meteorology and Climatology*

May 2021

Corresponding author:

Albeht Rodríguez Vega

Meteorological Institute of Cuba

Camagüey, Cuba

Email: albertrodriguezvega@gmail.com or albert@cmw.insmet.cu

Abstract

We present a climatological study of aerosols in four representative Caribbean islands based on daily mean values of aerosol optical properties for the period 2008- 2016, using the Aerosol Optical Depth (AOD) and Ångström Exponent (AE) to classify the dominant aerosol type. A climatological assessment of the spatio-temporal distribution of the main aerosol types, their links with synoptic patterns and the transport from different sources is provided. Maximum values of AOD occur in the rainy season, coinciding with the minimum in AE and an increased occurrence of dust, while the minimum of AOD occurs in the dry season, due to the predominance of marine aerosols. Marine and dust aerosol are more frequent in the easternmost islands and decrease westwards due to an increasing of continental and mixture dust aerosols. Therefore, the westernmost station displays the most heterogeneous composition of aerosols. Using a weather type classification, we identify a quantifiable influence of the atmospheric circulation in the distribution of Caribbean aerosols. However, they can occur under relatively weak and/or diverse synoptic patterns, typically involving transient systems and specific configurations of the Azores High that depend on the considered station. Backward trajectories indicate that dry-season marine aerosols and rainy-season dust are transported by air parcels travelling within the tropical easterly winds. The main source region for both types of aerosols is the subtropical eastern Atlantic, except for Cuba, where the largest contributor to dry-season marine aerosols is the subtropical western Atlantic. Different aerosol types follow similar pathways, suggesting a key role of emission sources in determining the spatio-temporal distribution of Caribbean aerosols.

Key words: AERONET, aerosols, aerosol optical depth, Ångström exponent, backward trajectories, weather types.

1. Introduction

Atmospheric aerosols, hereinafter aerosols, are solid or liquid particles suspended in the air, emitted directly from natural and anthropogenic sources (sea salt, mineral aerosol or dust, smoke, volcanic dust, etc.) or formed by gas-to-particle conversion as a result of chemical reactions. They have significant impacts on air quality and human health (e.g Kampa and Castanas, 2008; Monteil, 2008; Brunekreef, 2010; Cadelis et al., 2014). Additionally, aerosols play an important role in the radiative balance of the Earth's climate system, being regarded as one of the largest sources of uncertainty in climate models (e.g Zhang et al., 2012; Boucher et al., 2013; Myhre et al., 2013). The extinction and absorption of solar radiation are the main direct effects of aerosols (Verma et al., 2015), while indirect effects are related to their action as condensation nuclei and ice nuclei, causing modifications to the microphysical properties and lifetimes of clouds (Lohmann and Feichter, 2005; Weigel et al., 2011).

The different sources and atmospheric mechanisms of transport and deposition of aerosols cause complex spatial patterns and temporal variations. Therefore, an adequate estimate of the aforementioned aerosols' effects requires detailed spatio-temporal distributions, which can be inferred from measurements of their physical, optical and chemical properties. Currently, aerosol properties can be measured and analyzed *in situ* by different instruments (e.g Aerosol Mass Spectrometer, Roberts and Nenes, 2005; Snider et al., 2006; Reddington et al., 2017), or by active or passive remote sensing instruments (Lidar, sun photometer, satellite sensors, etc.). Although ground-based instruments are only representative of a small area around the monitoring site, they provide continuous time series of observations with very high temporal and spectral resolutions (Bennouna et al., 2013; Kumar et al., 2017; Antuña-Marrero, et al, 2018). This type of measurements is especially useful for small islands, where satellite sensors cannot provide a good representation of aerosol conditions and properties, due to limitations of resolution to capture the islands' topography and coastlines (Levy et al., 2013).

The Caribbean region embraces the Caribbean Sea, its islands and the surrounding coasts. It is located to the southeast of the Gulf of Mexico and the North American mainland, east of Central America, and north of South America. Its climate has been described as dry-winter tropical (Magaña et al., 1999; Giannini et al., 2000; Curtis, 2002; Mapes et al., 2005), with two main seasons in terms of rainfall patterns (dry and wet periods in November-April and May-October, respectively).

Regional studies have focused on the climatology and/or classification of aerosols for specific areas of the Caribbean. The first works in the region were those of Prospero et al. (1970) and Prospero and Carlson (1972). They focused on the transport of African dust across the Atlantic to the Caribbean, a topic further addressed in subsequent studies (Gioda et al., 2011; Spiegel et al., 2013; Fitzgerald et al., 2015; Denjean et al., 2016; Prospero and Diaz, 2016; Raga et al., 2016; Valle-Díaz et al. 2016; Velasco-Merino et al., 2018). In addition to African easterly waves, other synoptic patterns affect the atmospheric circulation over the Caribbean region. They include the Azores anticyclone, the Caribbean Low Level Jet, the Continental Anticyclone or polar low pressure systems (Jones et al, 2003; Fernández and Díaz, 2003; Cook and Vizy, 2010; Jury and Santiago, 2010; Chadee and Clarke, 2015; Sáenz and Durán-Quesada, 2015; Moron et al., 2016). However, studies linking weather patterns with aerosol types are scarce and limited to specific sites of the Caribbean. In the framework of the CARRIBA (Cloud, Aerosol, Radiation and tuRbulence in the trade wInd regime over BArbados) campaign, Wex et al. (2016) studied the transport of aerosols to Ragged Point

(Barbados), reporting three types of air masses. Jury (2017) determined the influence of meteorological conditions in air quality for La Parguera (Puerto Rico).

Current knowledge on the distribution of aerosol types in the Caribbean is spatially fragmented and based on short records. Estevan et al. (2011a) analyzed the evolution of aerosols in Camagüey (Cuba) for the period October 2008 to March 2009, which was characterized as a maritime mixed environment due to the abundance of marine and urban-polluted aerosols. Rivera et al. (2018) identified three different types of aerosols (clean marine aerosol, African dust and volcanic aerosol) in Cape San Juan Atmospheric Observatory (Puerto Rico). On the other hand, Kandler et al. (2018) described the microphysical properties and composition of mineral dust, sea salt and secondary compounds in Ragged Point (Barbados) during June-July 2013 and August 2016.

Therefore, previous research has mainly focused on dust transport from Africa and the concentration of different types of aerosols at specific sites. However, using aerosol measurements from a single station and short periods (sometimes less than a year) does not allow a comprehensive analysis of the distribution of aerosols, the heterogeneity of aerosol types across the region and the relative influence of different sources and meteorological patterns. In this paper we present a climatological study of aerosols in the Caribbean region for the period from 7 October 2008 to 31 December 2016 using measurements of four representative stations from the AErosol RObotic NETwork (AERONET), including an assessment of the main types of aerosols, their sources and transport, and the favorable synoptic patterns associated with their occurrence. The paper is structured as follows. In Section 2 AERONET data and the methodology are presented. The results of the aerosol climatology and classification, the source regions inferred from backward trajectories and the associated atmospheric circulation patterns are described in Section 3. Section 4 summarizes the main conclusions of this work.

2- Data and Method

2.1 AERONET data

AERONET is a worldwide network of ground-based sun photometers for the spatio-temporal monitoring of the aerosol's spectral optical properties in the total column of the atmosphere (Holben et al., 1998; Giles et al., 2019). Several studies describe in detail the instrumentation, data collection, retrieval algorithms and calibration procedures in AERONET network (Holben et al., 1998; Eck et al., 1999; Smirnov et al., 2000; Dubovik and King, 2000).

In this study we used daily mean values of Aerosol Optical Depth at 440nm (AOD_{440}), , and Ångström Exponent in the range from 440 to 870 nm ($AE_{440-870}$). The former is the most comprehensive single variable for the remote assessment of aerosol loading in the atmospheric column, while the latter is inversely related to the average size of the particles. Version 3.0 of the AERONET data products at the Level 2.0 (no clouds and total calibration with assured quality) was used in this study, which is available at https://aeronet.gsfc.nasa.gov/. Monthly and seasonal means, and their associated standard deviations, were computed from the daily means, with the dry and rainy season representing the November-to-April and May-to-October period, respectively. Four Caribbean stations from the AERONET database, representative of the Greater and Lesser Antilles and with a common measurement period (from 7 October 2008 to 31 December 2016) were selected: Ragged Point (Barbados), Guadeloupe, La Parguera (Puerto Rico) and Camagüey (Cuba; Figure 1). Table 1 summarizes relevant information of these four stations, including the geographical locations, distance to the sea and the main continental areas, as well as the number of days with available daily mean data for the analyzed period. Cloud-free days set the conditions to perform aerosol measurements and could bias the statistics of aerosols if the frequency of cloudy days is high. However, cloud-free conditions account for more than two thirds of the days in all stations (Table 1) and, overall, they experience relatively small variations (~10% in the mean) across the year and sites.

2.2 Aerosol type classification

Several studies have employed AERONET data to identify specific aerosol types. Typically, the basic parameters used to classify the aerosol type are AOD and AE (e.g Hess et al., 1998; Eck et al., 1999; Kaskaoutis et al., 2007; Toledano et al., 2007), or some parameters derived from the AERONET inversion algorithms (e.g. Dubovik and King, 2000). AOD at a wavelength of 500 nm is frequently employed, but this was not available at all sites during the period of analysis. For this reason, herein the discrimination of aerosol types was conducted for each station using only daily mean values of AOD_{440} and $AE_{440-870}$. This approach allows us identifying the dominant aerosol type for all days with available measurements, while inversion products only classify days with AOD values greater than 0.4.

It is not straightforward to determine the optimal thresholds of AOD_{440} and $AE_{440-870}$ that discriminate the different aerosol types due to their continuous distributions. Hence, we have used a hybrid approach based on a review of thresholds proposed in previous studies (e.g. Dubovik et al., 2002; Toledano et al., 2007; Holben et al., 2001; Kaskaoutis et al., 2007, Raptis et al., 2020) , as summarized in Table S1, combined with statistical analyses of the frequency distributions of AOD_{440} and $AE_{440-870}$. Distinctive modes in their distributions can indicate the presence of different aerosol types (O'Neill et al., 2000; Boselli et al., 2012). Therefore, we applied a Gaussian mixture model in order to identify multiple normal distributions embedded in the distributions that can be associated with specific aerosol types. The Gaussian mixture fits were computed for the $lnAOD_{440}$ and $AE_{440-870}$ distributions. Note that the same station can display a different number of modes in the $lnAOD_{440}$ and $AE_{440-870}$ distributions, because they measure different properties of the aerosol, therefore yielding complementary information for the assessment of the aerosol type. We also evaluated the joint AOD_{440} - $AE_{440-870}$ frequency distributions and compared the regions of high density in the AOD-AE space with the thresholds proposed elsewhere.

2.3 Weather types

To address the influence of the large-scale atmospheric circulation in the occurrence of aerosol types at the Caribbean stations, we employed a weather type classification, which assigns each day to a predefined synoptic pattern. Objective clustering techniques have been used in this region to classify the atmospheric circulation into a manageable number of recurrent weather patterns (e.g. Sáenz and Durán-Quesada, 2015; Moron et al., 2016). Following these studies, weather types were obtained from a k-means clustering of the first 15 Principal Components (85% of the total variance) applied to standardized daily anomalies of geopotential height (Z850) and wind vector at 850 hPa over the domain [5, 50] ºN and [10, 120] ºW. The analysis was performed for each season separately, using 100 iterations and 500 repetitions in order to retrieve robust clusters. The number of weather types must be chosen a priori, and previous studies on the Caribbean have shown that 8-to-11 weather types can capture the diversity and seasonal variations of synoptic conditions throughout the year (Sáenz and Durán-Quesada, 2015; Moron et al., 2016). Based on the analysis described in Appendix A, we retained four weather types for each season, in overall agreement with the number of seasonal weather types reported in the aforementioned studies and in Schultz et al. (1998) for the winter season.

To quantify the links between specific synoptic patterns and aerosol types, we computed for each station the fraction of days dominated by a given aerosol type and weather type, $P_{a,w}$. If weather conditions and aerosol types were independent, this probability should be equal to P_w, the climatological probability of occurrence of the weather type w. The ratio of these probabilities quantifies the change in the occurrence of that aerosol type for that weather type, as compared to the expected one. The significance of $P_{a,w}$ is addressed with a two-tailed binomial test.

2.4 Aerosol Transport and Backward trajectories

HYSPLIT Version 4.7 was used to determine the trajectory and origin of air masses associated with different types of aerosols at each station (Draxler and Hess, 1997). The model was initialized at 18 UTC (13:00 local time) using the NCEP/NCAR Reanalysis-1 (Kalnay et al., 1996). A preliminary evaluation of the NCEP/NCAR variables employed for the initialization of the HYSPLIT model confirmed the good performance of this reanalysis in the troposphere (not shown), as compared to observed profiles (2008-2009) from 15 Caribbean stations of the Integrated Global Radiosonde Archive (IGRA). Although aerosols are frequently transported below 1000 m, dust can also travel at higher levels (Wex et al., 2016; Rittmeister et al., 2017; Rivera et al., 2018). Therefore, backward trajectories were initialized at 500, 1500 and 3000 m a.g.l. of each station. For each station, level and day of the analyzed period, one backward trajectory spanning a 7-day interval was retrieved. The time step of the model's run was 1 hour, leading to 168 hours of backward flight time over the 7-day period and 3008 trajectories for each station and level.

To identify the most frequent source regions of the air masses, we followed the methodology of Toledano (2005) and Toledano et al. (2009), which uses predefined sectors for the source regions, considering the dominant synoptic patterns that affect the Caribbean region. These sectors are defined within the domain [5, 50] ºN and [10, 120] ºW and aim to identify air masses with different characteristics, as described in Table S2. The time of permanence of the air parcel over each predefined zone during its 7-day flight time was used to assign the trajectories to a given source region, assuming that the air parcel acquires the properties of the zone it crosses. Thus, for each day and station, we determined the number of time steps of its backward trajectory residing in each zone, so that the dominant aerosol type of that day was assigned to the source region displaying the maximum residence time. This daily classification was applied to the backward trajectories of each vertical level separately.

Figure 1 shows the six source regions of air masses for the classification of the backward trajectories. As the arrival of air masses to the Caribbean islands from these source regions is driven by the atmospheric circulation, our assessment of the dominant source regions can also be used to infer distinctive synoptic patterns related to the occurrence of aerosol types at each Caribbean station.

To better interpret the synoptic conditions associated with the long-term transport of different types of aerosols, we selected the days with a given aerosol type at each Caribbean station and computed composites of Z850 and wind vector fields at 850 hPa. Anomalies are defined with respect to the daily climatology of the 2008-2016 period. As compared to the backward trajectories, these composites correspond to the day of the aerosol arrival at the given station and hence they do not represent the mean atmospheric circulation for the 7-day period of the backward trajectory. In doing so, we retain synoptic features that would be filtered out by averaging over the 7-day backward trajectory. The significance of the composites was assessed using a bootstrap test of 1000 trials, each one containing the same number of cases as in the composite but selected randomly from the available days of each analyzed season. The composite and backward trajectory analyses were carried out for each season separately.

3. Results

3.1 Aerosol type characterization

3.1.1 AOD_{440} and $AE_{440-870}$ distributions.

Figure 2 shows the climatological monthly means of AOD_{440}. All stations show annual mean values of about 0.16, with a standard deviation of ~0.1 (Table 2). The annual cycle is characterized by a marked increase during the rainy season, which peaks in June-July for all stations, being less pronounced in Camagüey, where a second maximum occurs around April. Lower values are observed during the dry season for all stations, with minima in December. The highest standard deviations are also observed in the rainy season, with comparable ranges of interannual variability for all stations, slightly lower in Camagüey.

Figure 3 shows the frequency distributions of daily AOD_{440}, with the modes derived from the Gaussian mixture model. In Guadeloupe and La Parguera the distributions have similar shape, and are very well described (R^2=0.99) by the combination of two normal distributions. These preferred modes correspond to AOD_{440} ranges (mean ± standard deviation) centered at 0.08 ± 2.89 and 0.29 ± 3.63 in Guadaloupe and at 0.08 ± 2.39 and 0.22 ± 3.74 in La Parguera. At both sites the first mode (AOD_{440}~0.08) is dominant and reflects background aerosol loading (marine aerosol). The second mode (AOD_{440} ~ 0.22-0.29) corresponds to large aerosols such as dust episodes, which have been identified in these stations of the Caribbean (Section 1, Estevan et al. 2014; Prospero et al., 2014; Groß et al., 2016; Prospero and Diaz, 2016).

The $lnAOD_{440}$ distribution in Ragged Point fits well (R^2=0.99) to three normal distributions centered at AOD_{440} values of 0.06 ± 1.42, 0.19 ± 2.07 and 0.24 ± 2.83. The first and third modes match with those found in Guadeloupe and La Parguera, and are therefore representative of marine and dust aerosols, respectively. The second distinct mode has AOD_{440} values in between and could be related to marine mixed aerosols (Estevan et al., 2011a, Toledano et al., 2007).

The $lnAOD_{440}$ distribution of Camagüey is well described (R^2=0.99) by the sum of four normal distributions centered at AOD_{440} values of 0.12 ± 2.39, 0.18 ± 2.56, 0.33 ± 1.12 and 0.41 ± 2.64. The first and more recurrent mode has AOD_{440} values larger than 0.10 (the marine mixed aerosol ranges found in the other stations), whereas the two largest modes are characteristic of dust aerosol and high aerosol extinction (biomass burning), respectively (Boselli et al., 2012, Che et al., 2013). The second mode, between the marine mixed and dust aerosol peaks, is more characteristic of polluted or mixture dust aerosols, defined as the mixture of dust with marine, polluted or biomass burning aerosols (Clarke et al., 2004; Ansmann et al., 2011; Groß et al., 2011; Tesche et al., 2011).

The annual cycle of $AE_{440-870}$ (Figure 4) is opposite to that of AOD_{440}, with the largest values in the dry season (recall that large values of $AE_{440-870}$ correspond to fine aerosols). Overall, the standard deviation is also larger in the dry season for all stations, although this is less evident in Camagüey and La Parguera, which are also the stations with higher $AE_{440-870}$ all year round (Table 2). The areal extent of these islands and their proximity to the continent (Table 1) favor aerosol loading with high $AE_{440-870}$ (i.e. continental, polluted and/or biomass burning) emitted from local and continental sources.

The frequency distributions of $AE_{440-870}$ shows positive skewness in Ragged Point, Guadeloupe and La Parguera (Figure 5). In these stations, the $AE_{440-870}$ distributions are well described (R^2 = 0.99) by a Gaussian mixture model with two modes. In Ragged Point and Guadeloupe, the most recurrent mode (more than 80% of the observations) causes an asymmetric distribution, and its small $AE_{440-870}$ values (0.18 ± 1.45 and 0.17 ± 1.50, respectively) suggest a strong influence of coarse mode particles (sea salt and dust). The frequency distribution of $AE_{440-870}$ in these two stations decreases markedly, leading to about 5% of days with $AE_{440-870}$ above 1.0, which are embedded in the second mode (0.46 ± 1.95 and 0.99 ± 1.86 in Ragged Point and Guadeloupe, respectively). This second mode reflects aerosols dominated by fine mode particles such as continental, biomass burning and polluted aerosols. The comparatively longer right tail in Guadeloupe suggests the presence of different types of small size aerosols.

The two dominant modes of $AE_{440-870}$ in La Parguera (0.27 ± 1.54 and 0.62 ± 2.22) are close to the ranges found in Ragged Point and Guadeloupe for coarse and fine aerosols, although they exhibit distinct rates of incidence, yielding a linear decreasing frequency distribution. Despite being close to a Gaussian, the $AE_{440-870}$ distribution in Camagüey can also be approximated (R^2 = 0.99) to a bi-modal distribution distinguishing the coarse and fine modes with centers at 0.49 ± 1.95 and 1.08 ± 2.32. However, the mode with higher $AE_{440-870}$ values dominates the distribution, and this marked difference with the other stations suggests a larger influence of anthropogenic activities. Indeed, the highest frequency of $AE_{440-870}$ values between 1.0 and 1.5 occurs in Camagüey (34%), followed by La Parguera (13%), and typically correspond to intrusions of continental or mixture dust aerosols (Eck et al., 2010; Burgos et al., 2017). The few cases with $AE_{440-870}$ above 1.5 (e.g. polluted, biomass burning aerosols) are also more frequent in Camagüey.

Overall, the low annual mean AOD_{440} implies a predominance of marine aerosols in the Caribbean. However, the presence of seasonal variations in AOD_{440} and $AE_{440-870}$ suggests changes in the relative abundance of aerosol types throughout the year, with lower AOD_{440} / higher $AE_{440-870}$ values characteristic of continental, polluted or biomass burning aerosols in the dry season, and higher AOD_{440} / lower $AE_{440-870}$ values typical of dust aerosols in the rainy season. The magnitude of this seasonal cycle varies across stations, likely reflecting spatial variations in the frequency of different aerosol types.

3.1.2 AOD_{440} - $AE_{440-870}$ density plots.

A better characterization of the aerosol type can be done using AOD_{440}-$AE_{440-870}$ scatter plots (Figure 6; Kaskaoutis et al., 2007, Toledano et al., 2007; Kaskaoutis et al., 2011). In all the stations the scatter plot shows a high frequency of measurements in the region with $AOD_{440} \leq 0.18$ and $AE_{440-870} \leq 1.5$, which concentrates ~50% of the total cases in Camagüey and ~70% in the others stations. Pure marine aerosols have been associated with $AOD_{440} \leq 0.15$ and $AE_{440-870}$ values from 0 to 1.05 (Smirnov et al., 2002, Kambezidis and Kaskaoutis, 2008; Toledano et al., 2007; Estevan et al., 2011a, 2014; Bennouna et al, 2016), although this region in the 2D space is not free of continental influences (Hamilton et al., 2014; Wex et al., 2016). Indeed, other studies have also identified marine environments mixed with other types of aerosol, including continental ($AOD_{440} < 0.18$ and $AE_{440-870}$ from 0.7 to 1.05) and dust aerosols (AOD_{440} between 0.15 and 0.18 and $AE_{440-870} \leq 0.7$; Estevan et al., 2011a, Toledano et al., 2007). All these regions are well sampled in the diagrams of Fig. 6, and hence, the Caribbean can be regarded as a mixed marine environment.

A secondary maximum of AOD_{440}-$AE_{440-870}$ pairs is located in the lower right part of the diagrams, with high AOD_{440} (> 0.18) and low $AE_{440-870}$ (≤ 0.7) values, which typically correspond to pure dust aerosols (Velasco-Merino et al., 2018; Estevan et al., 2014; Groß et al., 2016; Weinzierl et al., 2017). Similar $AE_{440-870}$ thresholds have been employed in previous studies of dust transport from North Africa to the Caribbean (e.g. Estevan et al., 2011b, 2014; Velasco-Merino et al., 2018), although they are not very well constrained, likely due to changes in the size distributions of dust aerosols during their long-term transport (Maring et al., 2003). In addition, pure dust aerosols can be mixed with industrial or polluted aerosols and biomass burning aerosols increasing their $AE_{440-870}$, so that the region with AOD_{440} > 0.18 and 1.5 ≥ $AE_{440-870}$ > 0.7 is often regarded as of mixed dust aerosols (Estevan et al., 2011b; Raga et al., 2016; Velasco-Merino et al., 2018).

The relatively high density of AOD_{440}-$AE_{440-870}$ pairs in the upper half of the diagrams reflects the occurrence of continental, polluted and biomass burning aerosols. Within this region, AOD_{440} ≤ 0.18 and $AE_{440-870}$ > 1.05 pairs are typical of clean continental areas (Bennouna et al, 2013, 2016; Patel et al., 2017; Boiyo et al., 2018; Holben et al., 2001) or other fine mode aerosols with high $AE_{440-870}$ values, such as gases from volcanic emissions (Sears et al., 2013; Sellitto et al., 2018). The so-called urban or polluted aerosols also present high values of $AE_{440-870}$(Hess et al., 1998; Holben et al., 2001; Toledano et al., 2007) and are identified in the region with AOD_{440} between 0.18 and 0.35 and $AE_{440-870}$ > 1.5 in Fig. 6. Meanwhile, biomass burning aerosols are characterized by AOD_{440} > 0.35 and $AE_{440-870}$ > 1.5, typical of a turbid atmosphere with many fine particles (O'Neill et al., 2002; Eck et al., 2003).

Table 3 summarizes the thresholds used to classify the dominant aerosol type for each station. They have been selected taking into account the previous scatter plots, frequency distributions and the references cited above. These thresholds are similar to those employed in previous studies of the Caribbean (Estevan et al., 2011a, 2011b, 2014; Groß et al., 2016; Raga et al., 2016; Weinzierl et al., 2017; Velasco-Merino et al., 2018; see Table S1). The stations used in this study have AOD-AE distributions that share some characteristics, despite their differences in geographical location and/or size of the island where they are placed. This suggests similarities in the overall distribution of aerosol types across the Caribbean, supporting the choice of the same thresholds for all stations.

3.2 Spatio-temporal distribution of aerosol types

To explore in more detail the spatio-temporal distribution of aerosol types in the Caribbean, we have computed their relative frequencies (in percentage of days; Table 4) for all stations, following the classification of Table 3. Although there is always some degree of speciation, this approach allows us to assign each day to the dominant aerosol type.

Caribbean aerosols are mainly of marine origin. The proximity to the sea of Ragged Point, Guadeloupe and La Parguera stations is in agreement with their high frequency of marine aerosols (~70% of the days), while in Camagüey (the farthest station from the sea) they occur ~48% of the time. Dust aerosol is the second most important type in all stations (frequencies exceeding 20%), except in Camagüey, where continental aerosols represent the second most frequent type of aerosol. As dust in the region is frequently associated with Saharan episodes (Petit et al., 2005; Doherty et al., 2008; Estevan et al., 2014; Velasco-Merino et al., 2018), the number of days with this aerosol is conditioned by the geographical position of the island with respect to Africa, leading to higher frequencies in the easternmost stations.

Together, marine and dust aerosols account for about two thirds of the days, with differences across sites that range from almost ~60% in Camagüey to ~99% in Ragged Point. Indeed, the comparison across stations reveals a spatial gradient, with higher frequencies of these aerosols in the southeast. The reduced occurrence of these aerosols towards the Gulf of Mexico and North America is mainly compensated by an increasing frequency of continental and mixture dust aerosols, which are rare in the southeast (e.g. <1% in Ragged Point) but not in the northwest (e.g. ~20% each in Camagüey). The contribution of local sources (agricultural activity, natural landscape areas, etc.) to continental aerosols is expected to be low in small islands (Ragged Point and Guadeloupe), and comparatively greater in La Parguera and Camagüey. Therefore, the proximity of the islands to the main continental areas and their sizes explain well the unequal load of continental aerosols across sites (and its relative importance with respect to marine aerosols). The specific contribution of these factors is difficult to quantify, since the islands that are closer to North America are also the larger ones.

The presence of other aerosol types (mixture dust, polluted and biomass burning) is also affected by the size of the island (larger for La Parguera and Camagüey stations), as well as agriculture and other human activities (traffic, land use, etc.). Ragged Point and Guadeloupe report very few or no cases of polluted and biomass burning aerosols, although sometimes they can be transported within dust layers from Africa and the Amazonia during the dry season, being detected as mixture dust aerosols (Haywood et al., 2004; Kaufman et al., 2005; Ansmann et al., 2011; Wex et al., 2016; Jury, 2017). As a consequence of all these factors, Camagüey displays the most heterogeneous composition of aerosols, and is also the only site with a non-negligible (albeit very small, ~5% of the days) occurrence of atmospheric turbid conditions (either polluted or biomass burning aerosols).

The long upper tail of the $AE_{440-870}$ distribution in Guadeloupe can be associated with other marginal sources of fine mode particles (e.g. volcanic eruptions). Such is the case of the episode of extreme continental aerosols detected therein between 27 September 2010 and 2 February 2011, which coincides with volcanic gas emissions from Soufrière Hills (Montserrat; MVO Activity Reports 2010) located at ~80 km from the station. In La Parguera and Camagüey, extreme continental aerosols were also observed several days after active episodes of the Soufrière Hills volcano (e.g. in May 2012 and in October 2010, respectively; MVO Activity Reports 2012, 2013). We did not identify additional matches with volcanic activity within the region. Therefore, volcanic aerosols will not be considered separately from continental aerosols in the subsequent analyses.

The monthly frequency distributions of aerosol types reveal clear seasonal cycles frequency distributions (Figure 7). Marine aerosols are more frequent in the dry season, occurring in more than half of its days. There are differences among sites in the amplitude of this annual cycle, which is more pronounced for the stations with a larger contribution of marine aerosols (Ragged Point and Guadeloupe). The dry season also concentrates the highest frequencies of continental aerosols, which tend to show an annual maximum in autumn.

The decrease of marine and continental aerosols in the rainy season is partially compensated by an increase of dust aerosols, which display a pronounced peak between June and August (often exceeding 50% of the days), and a clear minimum in the dry season, with <10% of days between December and February for all sites. This annual cycle is opposite to that of marine aerosols, suggesting an anticorrelation between them. Indeed, the amplitude of the annual cycle of dust is also larger in the stations with higher abundance of marine aerosols. The seasonality of dust aerosols is in agreement with that reported for dust emissions in northern Africa (Middleton and Goudie, 2001; Goudie and Middleton, 2006), which shows minimum activity in October-December, coinciding with the lowest loading of dust aerosols in the Caribbean region. The emission of African dust aerosols starts to increase in January, reaching the highest concentrations in April-June over the southern region of the Mauritania and Mali, and in July-September over western Sahara and southern Morocco. The transatlantic transport of dust plumes from these two major source areas is linked to strong convective disturbances and easterly waves crossing the North Atlantic within 5-7 days (Middleton and Goudie, 2001).

Finally, polluted aerosols (only present in La Parguera and Camagüey) do not have a well-defined seasonal distribution, whereas mixture dust and biomass burning aerosols tend to display larger frequencies in the dry season (when the biomass moisture is low and forest fires are more frequent). However, the number of cases of these aerosols is low to retrieve robust estimates, exception made for mixture dust at Camagüey. Indeed, episodes of biomass burning aerosols can be observed outside of the dry season, as during the severe drought of 2012 in Camagüey.

3.3. Weather types associated with Caribbean aerosols.

To explore the links between atmospheric circulation and aerosol types we used a cluster-based classification of synoptic patterns (Section 2.3). Figures 8 and 9 show the main four weather types for the dry and rainy season, respectively. Differently to composite analyses, weather types do not emphasize the atmospheric circulation signatures associated with the occurrence of Caribbean aerosols (which may be favored by different weather types). However, they provide a useful tool to assess whether recurrent patterns play a role and how it varies across aerosol types and stations. This is evaluated by comparing the likelihood of occurrence of aerosol types under different synoptic patterns, as shown in Figure 10.

During the dry season, marine aerosols are more likely to occur under weather type 3, which displays positive anomalies of the Continental North America Anticyclone and weakening of the Azores High (Fig. 8). This weather type comprises ~25% of all days, but ~40% of the days with marine aerosols, which represents a 66% increase in its probability of occurrence ($p<0.01$ after a binomial test; Fig. 10a). This weather regime cannot account for the high frequency of marine aerosols that characterize the dry season. Weather type 1 comprises an additional fraction of days with marine aerosols (~20% for all stations), which is higher ($p<0.01$) than the climatological occurrence of that weather type (~15%). Interestingly, this weather type shows some signatures that oppose to those of weather type 3, in particular a weakening of the Continental North America Anticyclone and a contraction and intensification of the Azores High (Fig. 8). These results suggest that the weather types do not fully capture the key signatures associated with marine aerosols or that the synoptic patterns can change from case to case. Regardless of the cause, the analysis shows a quantifiable (and statistically significant) influence of the atmospheric circulation. As a matter of fact, the probability of occurrence of marine aerosols decreases significantly ($p<0.01$) in all stations under weather types 2 and 4, indicating that these synoptic conditions are indeed unfavorable (Fig. 10a).

The frequency of other aerosol types in the dry season also tends to be higher during weather types 1 and 3, suggesting that the same synoptic pattern can promote different aerosol types, although the assessment is hampered by the low number of cases in some stations. Their degree of influence varies across stations, though. In particular, there is a tendency for continental, dust and mixture dust aerosols to be more likely in the northern stations under weather type 3 (probability changes >50%), whereas weather type 1 is more favorable than weather type 3 for these aerosols in the southern stations. Another remarkable (although non-significant) aspect concerns dust aerosols in the northern stations, which are also favored by weather type 2, characterized by a pronounced intensification of the Continental North America Anticyclone. These results suggest that, different to the southern stations, the few dust episodes reported in Camagüey and La Parguera during the dry season may be associated with emissions from North America.

The four clusters of the rainy season (Fig. 9) are substantially different from those of the dry season. Overall, they are associated with strengthened (cluster 1) or weakened (cluster 4) signatures in the northern flank of the Azores High, or shifted states (reflecting an expansion, cluster 3 or contraction, cluster 2) of the anticyclone. As in the dry season, we find two favorable weather regimes (1 and 4) for the occurrence of Caribbean aerosols, which are detected across aerosol types (Fig. 10b). The other two weather types tend to be unfavorable, to a varying extent depending on the station and/or type of aerosol ($p<0.01$ for marine and dust aerosols). Weather type 4 is associated with a pronounced increase (~80% or higher) in the probability of occurrence of marine and dust episodes in all stations ($p<0.01$), although in Camagüey the largest increases in these aerosols are reported for weather type 1 (~90%). Moreover, weather types 4 and 1 can, respectively, double the probability of occurrence of continental and mixture dust aerosols where they occur (i.e. La Parguera and Camagüey, $p<0.01$), and they are also the preferred patterns for the few cases of polluted and biomass burning in Camagüey. Similar to the dry season, these weather types correspond to somehow opposite atmospheric circulation patterns, although they both reflect synoptic departures of the Azores High. Note that days with the same aerosol type are often detected in a row (in the form of episodes). Therefore, a feasible explanation is that the same aerosol episode can occur under different weather patterns as the synoptic disturbance promoting its transport travels along the Atlantic. This also applies to the dry season, for which synoptic perturbations in the northern flank of the Azores High and the Continental North America anticyclone are the key features associated with Caribbean aerosols. Overall, the results motivate a lagrangian-based description of aerosol episodes.

3.4 Transport and source regions of Caribbean aerosol types

In this section we characterize the large-scale transport of different types of Caribbean aerosols using composites of the atmospheric circulation in the lower troposphere (Z850 and wind vector anomalies at 850 hPa) and backward trajectories. We mainly focus on marine aerosols in the dry season (Figure 11) and dust in the rainy season (Figure 12), since they are the only combinations with enough number of cases in all stations (Fig. 7). Similar patterns of the composites of the atmospheric circulation are observed in the middle and upper troposphere (500 hPa and 250 hPa, Fig. S1 and S2).

As they dominate in the respective seasons, the number of days for the composites is very high, and would lead to overall weak anomalies and autocorrelation issues by the occurrence of successive days with the same aerosol type. Including all days of the same episode in the composite may also mask key synoptic features (e.g. travelling disturbances) due to the transient nature of the atmospheric circulation. Therefore, the composites only include the first day of independent events, defined as those of any duration separated by at least five days. Accordingly, if there are several occurrences of a given aerosol type within a five-day interval at a given station, the first day is only considered.

For coherence, the composited trajectories are also computed using only the 7-day backward trajectory for the first day of these episodes (the results are similar if all days with the same aerosol type are considered; not shown). That way, the first day of the composited trajectory corresponds to the onset of aerosol episodes at the given station, and the remaining backward trajectory reports the transport of that aerosol type. To assess the robustness of the composited trajectories, Figure S3 shows the density of backward trajectories at different heights for the first day of all episodes of marine and dust aerosols included in the composites of the dry and wet seasons, respectively. The source region is determined for each episode by assigning this 7-day backward trajectory to one of the predefined regions defined in Fig. 1, attending to its time of residence (see Section 2.4). The main source regions of different aerosol type episodes are summarized in Figure 13.

3.4.1 Dry season.

The occurrence of marine aerosols in the Caribbean is associated with synoptic disturbances in the northern flank of the Azores High, often involving the passage of extratropical cold fronts (Fig. 11). This is supported by composites for different lags with respect to the day of the aerosol arrival at each station (not shown), which reveal travelling synoptic perturbations, as well as by composites at upper levels (Figure S1). As a result, the composited fields of Fig. 11 tend to display significant anomalies with respect to the climatology over small regions. Despite this, there is some tendency for a zonal confinement and/or rearrangement of the Azores High, sometimes accompanied by anomalies of the Continental Anticyclone over North America, in agreement with the analysis of weather types (Section 3.3).

In the westernmost stations (La Parguera and Camagüey) there is a pronounced regional strengthening of the Continental Anticyclone (Figs. 11c, d). In Camagüey, where marine aerosols are less frequent, the results suggest an additional weakening of the Azores High and positive Z850 anomalies confined to western Caribbean and the east coast of the United States. Differently, the easternmost stations (Ragged Point and Guadeloupe) tend to show an overall weakening of the Continental Anticyclone, accompanied by positive Z850 anomalies over the northern flank of Azores high in the case of Guadeloupe (Figs. 11a, b). Interestingly, the composites for the farthest stations (Camagüey and Ragged Point) share a weakening of the Azores High, whereas the stations in between (La Parguera and Guadeloupe) rather display an intensification and/or zonal extension. This suggests that the occurrence of marine aerosol episodes is strongly sensitive to the specific location of the station and/or its relative position with respect to the Azores High. As marine episodes can affect one island after the other as they travel, the composites might reflect different snapshots of the same atmospheric disturbance traveling westward and affecting the westernmost stations of La Parguera and Camagüey when it reaches North America (see also Fig. S1). This would also explain why days with the same aerosol type at a given station can be associated with opposite weather types (Fig. 10a; Section 3.3).

The inspection of backward trajectories (Fig. S3 Left Panel) and their composite (colored lines in Fig. 11) confirms that the air parcels originate in the subtropical Atlantic, moving southwards before veering to the west towards the Caribbean stations. As one proceeds from the southern to the northern stations, air parcels have closer origins and travel shorter distances, following the westward movement of the atmospheric disturbances. These results stress the importance of regional anomalies of the Azores High, which allow subtropical air masses being either trapped within the trade winds and transported to the Caribbean or recirculated within the Caribbean itself in the case of Camagüey. The mean height of the air parcels arriving at 500 m increases backwards in time for all stations, and the same behavior is observed for higher arrival heights (not shown). The different pathways between the backward trajectories at the three vertical levels (Fig. 11) support the strong baroclinic environment typical of synoptic travelling disturbances.

In agreement with the composites, the principal source region of marine aerosols in the Caribbean is Zone V (eastern subtropical Atlantic), which is associated with maritime air masses transported by enhanced easterly winds towards the region (Fig. 13 Left Panel). This configuration is typical of the Caribbean and can occur all year round (Jones at al., 2003; Jury and Santiago, 2010). The contribution of this zone is dominant for more than 70% of the marine aerosol episodes in Ragged Point, and it decreases towards the western stations (less than 50% in Camagüey). Zone II (Caribbean) is the second largest source of marine aerosols for all stations (Fig. S3 Left Panel), although with a varying contribution. Camagüey and La Parguera have the highest contribution of this zone (>25%), which explains the decreasing influence of Zone V (Fig. 13 Left Panel). Therefore, the contribution of nearby sources of marine aerosols (Zone II) increases for the western stations. Overall, we do not identify systematic differences between the mean height of the backward trajectories associated with air masses coming from Zone II and Zone V (not shown).

The remaining aerosol types are either uncommon or biased to specific stations so as to retrieve robust composites for the entire Caribbean region. For stations with enough number of episodes (e.g. continental and mixture dust aerosols in Camagüey), the backward trajectories (Figure S4) and source regions (Fig. 13 Left Panel) do not reveal substantial differences with respect to those of marine aerosols. In particular, the subtropical eastern Atlantic provides the largest contribution to dust aerosols in Ragged Point, while nearby maritime (Zone II) and continental areas of North America (Zone I) are the main sources of continental and mixture dust aerosols in Camagüey (Fig. 13 Left Panel). The similar origin of the less common aerosol types may indicate that they can travel embedded in the same air parcels transporting marine aerosols.

3.4.2 Rainy season.

Dust episodes in the Caribbean during the rainy season are often associated with tropical easterly waves travelling from western Africa (Prospero et al., 2014; Weinzierl et al., 2017). The structure of these travelling disturbances agrees with a generalized tendency for Z850 rises over the considered station (Fig. 12) and the transient nature of the lagged (not shown) and upper-level composites (Figure S2). It also explains why the same aerosol type can be associated with different (eventually opposite) weather types (Section 3.3). Enhanced easterlies are also a common signature of dust episodes for all Caribbean stations, which are favored by slightly different configurations of the Azores High depending on the specific island. In particular, dust episodes in Guadeloupe and La Parguera are associated with a localized southwestern extension of the Azores High and the trade winds. Differently, the southernmost and northernmost stations display a generalized expansion and contraction of the Azores High, respectively, with hints of zonal dipole anomalies over the tropical Atlantic that are characteristic of easterly waves (Diedhiou et al., 1999; Middleton and Goudie, 2001; New and Estupiñán 2013).

The regional enhancement of easterlies leads to robust backward trajectories for the dust episodes of all stations (Fig. S3 Right Panel). The air masses travel from the eastern

Atlantic within the Azores High and are transported by the trade winds towards the Caribbean stations (Fig. 12), which supports the Saharan origin of the Caribbean dust episodes. There is a clear dominance of air masses from the tropical Atlantic (Zone V; contributions of ~70% for all Caribbean stations), being slightly higher for the southern stations (Fig. 13b). As in the case of marine aerosols of the dry season, the mean height of the air parcels decreases as they approach to the target station (not shown). However, the backward trajectories of dust episodes tend to follow more similar paths at different altitudes than those of marine aerosols (cf. Figs. 11 and 12). Assuming that the injection of dust can reach these upper levels and remain therein, this would lend support to the hypothesis of a long-term transport at a wide range of altitudes.

The main source of marine aerosols (the other dominant type of the rainy season) is also Zone V (Fig. 13b), particularly for the southern stations, and its contribution decreases towards the north, along with an increasing influence of the local Caribbean source (Zone II). Different to the dry season, the trajectories are more zonally elongated towards the eastern tropical Atlantic, and show stronger resemblance to the rainy season paths of pure dust (Fig. S3 Middle Panel). Therefore, marine and pure dust episodes follow similar preferred trajectories, suggesting that the type of aerosol can be determined by changes in the composition of the air parcels as they pass through activated emission sources rather than by their specific origin and path. This is supported by the assessment of the remaining aerosol types (Fig. 13b). Zone V is the main source region of the few cases of continental and mixture dust aerosols observed in Ragged Point, Guadeloupe and La Parguera. The only exception is Camagüey, where the occurrence of continental and mixture dust aerosols is dominated by Zone II, pointing to a North American origin. This region is also the leading source for the other marginal aerosol types detected in Camagüey (polluted and biomass burning aerosols).

As mentioned above, there are eventual aerosol episodes with extreme continental characteristics ($AE_{440-870}$>1.7). The inspection of their backward trajectories (red lines in Fig. S4) reveals that air parcels travelled close to the Soufrière Hills volcano (e.g. Guadeloupe and La Parguera events), or crossed the northeast coast of South America (most of the cases detected in Camagüey), likely linked to sulfur dioxide and other fine particles from the oil production industry.

4. Conclusions and discussion

This paper presents a climatological study of aerosols in the Caribbean region, including the classification of aerosol types and the synoptic patterns and backward trajectories associated with their transport. To this end, we have employed daily mean observations of Aerosol Optical Depth (AOD) at 440nm (AOD_{440}) and Ångström exponent at 440 and 870 nm ($AE_{440-870}$) from four representative stations of the AERONET dataset.

The annual cycle of Caribbean aerosols is characterized by a marked increase of AOD_{440} in the rainy season (April-October) and decreases in the dry season (November-March), with opposite variations of $AE_{440-870}$. Seasonality in the aerosol source regions and climatological features of the atmospheric circulation are the major drivers of these seasonal changes in aerosol loading and speciation. In particular, the distinctive rainy season signatures in the Caribbean are largely explained by the activation of African dust emissions, along with the predominance of trade winds and associated easterly waves in summer induced by seasonal changes in the configuration and position of the subtropical anticyclone. We note here that Camagüey shows a secondary peak of AOD_{440} during the dry season, in agreement with previous studies (García et al., 2015). A similar double peak has been reported in other regions with large contribution of polluted or dust aerosols such as the eastern United States (Zhao et al., 2018), Dakar and Cape Verde (Xian et al., 2020) and El Arenosillo, Spain (Toledano et al., 2007). Secondary peaks have also been detected in other Caribbean regions (e.g. Barbados and the Lesser Caribbean; Prospero and Nees 1986; Doherty et al. 2008) and attributed to dust. However, in Camagüey dust episodes are uncommon during the dry season, and continental air masses from North America with large contribution of anthropogenic aerosols would better explain its secondary peak, as in the eastern United States. A similar double peak is not observed in Ragged Point, Guadeloupe and La Parguera, arguably because dust aerosols typically follow the low-to-mid-level trade winds, which flow at lower latitudes during the dry season (Prospero et al., 2014; Xian et al., 2020).

Several aerosol types are observed in the Caribbean region. The multimodal frequency distributions of AOD_{440} and $AE_{440-870}$ show three fundamental groups, with a predominance of marine and dust aerosols (coarse group), followed by fine mode aerosols (polluted, continental and biomass burning aerosols) and the mixture of these two groups. Overall, the results indicate a predominance of coarse aerosols in the Caribbean throughout the year, resulting from higher abundances of marine aerosols in the dry season, and of dust aerosols in the rainy season. The frequency of days when these aerosols are dominant and the amplitude of their seasonal cycles vary across stations, modulated by the abundance of other secondary aerosol types (mainly continental and mixture dust). In particular, there is a spatial gradient in the distribution of coarse aerosols, which are more frequent in the easternmost islands, and decrease westwards. As such, Camagüey, and secondarily La Parguera display the most heterogeneous composition of aerosols, being the stations with the largest frequencies of continental, polluted and mixture dust aerosols, and the only ones with detectable biomass burning aerosols. The different frequencies of aerosol types across stations are to a large extent in agreement with their distances to the open sea, as well as the geographical location (proximity to North America) and spatial extension of their islands. Local sources (agriculture, traffic) and/or sporadic natural phenomena (e.g. volcanic emissions) could partially explain some of the reported differences in the frequency distributions of AOD_{440} and $AE_{440-870}$ (degree of asymmetry, long tails, etc.). Overall, marine and continental aerosols are more frequent in the dry season and decrease towards the rainy season, when dust aerosols dominate. The latter does not mean an influence of dust aerosols in the occurrence of cloudy days, which does not display an obvious annual cycle over the Caribbean. The annual maxima of dust aerosols do not agree with the climatological peaks in precipitation either, which tend to occur in May-June for Camagüey and La Parguera, but in October for Ragged Point and Guadeloupe (Taylor and Alfaro, 2005; Martinez et al., 2019). Indeed, dust aerosols can inhibit cloud formation and precipitation, because they are usually accompanied by dry air masses (Goudie and Middleton, 2006). However, if this is the case, such effect is not reflected in the climatological precipitation patterns, either: Camagüey and La Parguera show mid-summer breaks in rainfall by late July - early August (when dust aerosols are more common), but the same is not observed in the stations with the largest frequencies of dust (Ragged Point and Guadeloupe). On the other hand, polluted aerosols do not have a well-defined seasonal distribution, whereas mixture dust and biomass burning aerosols tend to be more frequent in the dry season, although their low frequencies of occurrence prevent robust estimates.

The analysis of weather types demonstrates a quantifiable influence of the atmospheric circulation in the occurrence of Caribbean aerosols. Out of the four weather types of each season, we identify two favorable (and two unfavorable) synoptic patterns that are common for all aerosol types and stations. The degree of influence varies more with the station than with the type of aerosol considered, stressing the importance of the geographical location. In some cases, a specific weather type can double the probability of occurrence of an aerosol type. However, the same aerosol type can occur under weather patterns with very different (eventually opposite) signatures. This points to travelling synoptic disturbances at the core of the aerosol transport, with favorable weather types representing different stages of the long-term transport. Additional composite analyses indicate that the Azores High and the Continental Anticyclone over North America are the main drivers of the large-scale wind conditions favorable for the transport of aerosols to the Caribbean. The easterlies arise as the dominant wind component associated with the main Caribbean aerosols all year round. During the dry season, the synoptic patterns conductive to marine aerosols vary across the stations, but when considered together, they suggest transient baroclinic disturbances travelling westward through the northern flank of the Azores High. Accordingly, the same synoptic perturbation could instigate episodes of the same aerosol type at different Caribbean stations as it travels over the Atlantic. Similarly, the synoptic patterns associated with dust episodes during the dry season stress the importance of the trade winds and support the major role of easterly waves travelling from Northern Africa.

Backward trajectories confirm that marine aerosols in the dry season are transported in air parcels steered by a strengthened northwesterly flow over the North Atlantic towards the main trade belt. In the rainy season, dust is frequently transported by air parcels with zonal paths along the tropical easterly winds. As a consequence, the eastern Atlantic (Zone V) is the major source of marine and dust aerosols (the latter ultimately originating in Northern Africa). The contribution of this region varies with the considered station, being lower for the westernmost islands, which are more affected by local sources in the Caribbean (Zone II) and the surrounding areas (North America and subtropical northwestern Atlantic, Zone I). The determination of the main source regions for other aerosol types is hampered by the overall low number of episodes. However, the assessment of individual trajectories suggests similar origins (the eastern tropical Atlantic for continental aerosols in the easternmost stations, and a larger contribution of nearby sources in the westernmost islands). Nearby regions (the Caribbean and North America) also act as the main sources of the few episodes of biomass burning, polluted and mixture dust aerosols detected in the westernmost stations, as well as of some extreme continental episodes linked to either natural (volcanic emissions) or anthropogenic (industrial activities) sources. Overall, the similar trajectories and sources for the different aerosol types suggest that they could be transported by the same air parcels. According to this hypothesis, once the synoptic conditions initiate the transport, the type of aerosol would be largely influenced by changes in the composition of the air parcel as its travels over activated emission sources. Dedicated modeling studies accounting for the local and remote sources/sinks of each aerosol type and associated processes (chemical reactions, deposition, etc.) that intervene in the large-scale transport of air parcels would be required to achieve a more detailed understanding of the spatio-temporal distribution of aerosols in the Caribbean.

Acknowledgements. This research was supported by the CSIC ("Consejo Superior de Investigaciones Científicas" of Spain) under project COPA20207. We thank Jack Molinie, Joseph M. Prospero and Brent N. Holben for his effort in establishing and maintaining the Guadeloupe, Ragged Point and La Parguera AERONET sites. The sun photometer at Camagüey was provided by the *Grupo de Óptica Atmosférica* of the University of Valladolid (UVA), Spain under a cooperation agreement with INSMET, Cuba. The agreement signed in 2007, still in place until the present, has been successful despite limitations and obstacles (Antuña-Marrero et al., 2016; GOAC, 2020). Special recognition to Prof. Ángel de Frutos and Victoria Cachorro from UVA for supporting the joint research on atmospheric aerosols. Also, INSMET is recognized by its support until the present. Also, we would like to acknowledge NCEP/NCAR Reanalysis team for making the data publicly available. Version 3.0 of AERONET data were freely downloaded from the AERONET web site (https://aeronet.gsfc.nasa.gov, last access: 8 June 2020). NCEP-NCAR Reanalysis data were downloaded from (https://www.esrl.noaa.gov/psd/data/gridded/data.ncep.reanalysis2.html, last access: 25 Mayo 2018). We thank the Editor and three anonymous reviewers for their valuable comments and suggestions.

Appendix A

The optimal number of clusters for the rainy and dry seasons was determined using the classifiability index (CI, Michelangeli et al., 1995):

$$CI(k) = \frac{1}{M(M-1)} \sum_{1:m \neq m'}^{M} C\left(Pa_m(k), Pa_{m'}(k)\right)$$

where *C* measures the similarity (pattern correlation) between two different partitions out of *M* initial random seeds of *k* clusters. The analysis was applied to $M = 100$ classifications of *k* clusters, ranging from 2 to 20. A CI(*k*) value of 1 means that the *M* partitions yielded exactly the same *k* clusters. The CI distribution is compared to that obtained from a red noise process with a first order (lag-1 autocorrelation) autoregressive model, CI' (Figure A1). An optimal number of clusters is that preserving high CI*(k)* values and substantial departures from those of CI'*(k)*. Accordingly, we selected four weather types for each season.

References

Ansmann, A., A. Petzold, K. Kandler, I. Tegen, M. Wendisch, D. Müller, B. Weinzierl, T. Müller, and J. Heintzenberg (2011), Saharan Mineral Dust Experiments SAMUM-1 and SAMUM-2: What have we learned?, *Tellus B*, 63, 403–429, doi:10.1111/j.1600-0889.2011.00555.x.

Antuña-Marrero, J. C., A. De Frutos Baraja, and R. Estevan Arredondo (2016), Joint aerosol research between Cuba and Spain proves fruitful, *Eos*, **97**, https://doi.org/10.1029/2016EO060125. Published on 06 October, 2016.

Antuña-Marrero, J. C., V. Cachorro, F. García, A. M. de Frutos, A. Rodríguez, D. Mateos, R. Estevan, And C. Toledano (2018), Comparison of aerosol optical depth from satellite (MODIS), sun photometer and broadband pyrheliometer ground-based observations in Cuba, *Atmos. Meas. Tech.*, 11, 2279–2293, https://doi.org/10.5194/amt-11-2279-2018

Bennouna Y., V. E. Cachorro, B. Torres, C. Toledano, A. Berjón, A. de Frutos, I. Alonso Fernández-Coppel, (2013), Atmospheric turbidity and the annual cycle of aerosol optical depth over north-center Spain with ground (AERONET) and satellite (MODIS) remotely sensed data. *Atmos. Environ*. **67**, 352-364, doi.org/10.1016/j.atmosenv.2012.10.065

Bennouna Y.S., V.E. Cachorro, D. Mateos, M.A. Burgos, C. Toledano, B. Torres, A.M. de Frutos (2016), Long-term comparative study of columnar and surface mass concentration aerosol properties in a background environment, *Atmos. Env.* 140 (2016) 261-272, http://dx.doi.org/10.1016/j.atmosenv.2016.05.061.

Boiyo R., K. R. Kumar, T. Zhao (2018), Optical, microphysical and radiative properties of aerosols over a tropical rural site in Kenya, East Africa: Source identification, modification and aerosol type discrimination, *Atmospheric Environment,* **177,** 234–252, https://doi.org/10.1016/j.atmosenv.2018.01.018.

Boselli, A., R. Caggiano, C. Cornacchia, F. Madonna, L. Mona, M. Macchiato, G. Pappalardo, S. Trippetta (2012), Multi year sun photometer measurements for aerosol characterization in a Central Mediterranean site, *Atmos. Res.,* **104–105** 98–110, http://dx.doi.org/10.1016/j.atmosres.2011.08.002.

Boucher, O., D. Randall, P. Artaxo, C. Bretherton, G. Feingold, P. Forster, V.-M. Kerminen, Y. Kondo, H. Liao, U. Lohmann, P. Rasch, S.K. Satheesh, S. Sherwood, B. Stevens and X.Y. Zhang (2013), Clouds and Aerosols. In: Climate Change 2013: The Physical Science Basis. Contribution of Working Group I to the Fifth Assessment Report of the Intergovernmental Panel on Climate Change [Stocker, T.F., D. Qin, G.-K. Plattner, M. Tignor, S.K. Allen, J. Boschung, A. Nauels, Y. Xia, V. Bex and P.M. Midgley (eds.)]. *Cambridge University Press*, *Cambridge*, United Kingdom and New York, NY, USA.

Brunekreef B. (2010), Air Pollution and Human Health: From Local to Global Issues, *Procedia Social and Behavioral Sciences* 41, (2010), 6661–6669.

Burgos, M. A. , D. Mateos, V. E. Cachorro, C. Toledano, and A. M. de Frutos (2017), Aerosol properties of mineral dust and its mixtures in a regional background of north-central Iberian Peninsula. STOTEN 572, 1005-1019. http://dx.doi.org/10.1016/j.scitotenv.2016.08.001.

Cadelis G., R. Tourres, J. Molinie (2014), Short-Term Effects of the Particulate Pollutants Contained in Saharan Dust on the Visits of Children to the Emergency Department due to Asthmatic Conditions in Guadeloupe (French Archipelago of the Caribbean), PLoS ONE 9(3): e91136. doi:10.1371/journal.pone.0091136.

Chadee, X. T., and R. M. Clarke (2015), Daily near-surface large-scale atmospheric circulation patterns over the wider Caribbean, *Clim. Dyn.*, **44**, 2927-2946. DOI 10.1007/s00382-015-2621-2.

Che H., Y. Wang, J. Sun, X. Zhang, X. Zhang, and J. Guo (2013), Variation of Aerosol Optical Properties over the Taklimakan Desert in China, *Aerosol and Air Quality Research*, 13: 777–785, 2013, doi: 10.4209/aaqr.2012.07.0200.

Clarke A. D., Y. Shinozuka, V. N. Kapustin, S. Howell, B. Huebert, S. Doherty, T. Anderson, D. Covert, J. Anderson, X. Hua, K. G. Moore II, C. McNaughton, G. Carmichael, and R. Weber (2004), Size distributions and mixtures of dust and black carbon aerosol in Asian outflow: Physiochemistry and optical properties, *J. Geophys. Res.*, 109, D15S09, doi:10.1029/2003JD004378.

Cook, K. H., and E. K. Vizy (2010), Hydrodynamics of the Caribbean Low-Level Jet and Its Relationship to Precipitation, *J. Climate*, **23**, 1477-1494. http://dx.doi.org/10.1175/2009JCLI3210.1.

Curtis, S. (2002), Interannual variability of the bimodal distribution of summertime rainfall over Central America and tropical storm activity in the far-eastern Pacific, *Climate Res.*, **22**: 141–146.

Denjean, C., P. Formenti, K. Desboeufs, S. Chevaillier, S. Triquet, M. Maillé, M. Cazaunau, B. Laurent, O. L. Mayol-Bracero, P. Vallejo, M. Quiñones, I. Gutierrez, F. Cassola, P. Prati, J. A. Ogren, and E. Andrews (2016), Size distribution and optical properties of African mineral dust after intercontinental transport, *J. Geophys. Res. Atmos.*, **121**, 7117–7138, http://dx.doi.org/10.1002/2016JD024783.

Diedhiou A., S. Janicot, A. Viltard, P. de Felice, and H. Laurent (1999), Easterly wave regimes and associated convection over West Africa and tropical Atlantic: results from the NCEP/NCAR and ECMWF reanalyses, *Climate Dynamics* (1999) 15:795-822.

Doherty, O. M., Riemer, N., & Hameed, S. (2008). Saharan mineral dust transport into the Caribbean: Observed atmospheric controls and trends, *J. Geophys. Res.*, 113, D07211, https://doi.org/10.1029/2007JD009171.

Draxler, R. R., and G. D. Hess (1997), Description of the HYSPLIT_4 modelling system, *NOAA Tech. Memo.*, ERL ARL-224, 24 pp.

Dubovik, O., and M. D. King (2000), A flexible inversion algorithm for retrieval of aerosols optical properties from sun and sky radiance measurements, *J. Geophys. Res.*, **105**, D16, 20,673-20,696.

Dubovik O., B.N. Holben, T.F. Eck, A. Smirnov, Y.J. Kaufman, M.D. King, D. Tanré, I. Slutsker (2002), Variability of absorption and optical properties of key aerosol types observed in worldwide locations. *J. Atmos. Sci.* **59**: 590–608.

Eck, T. F., B. N. Holben, J. S. Reid, O. Dubovik, A. Smirnov, N. T. O'Neill, I. Slutsker, and S. Kinne (1999), Wavelength dependence of the optical depth of biomass burning, urban, and desert dust aerosols. J. Geophys. Res. **104**, 31333–31349.

Eck T.F., B.N. Holben, J.S. Reid, N.T. O'Neill, J.S. Schafer, O. Dubovik, A. Smirnov, M.A. Yamasoe, P. Artaxo (2003), High aerosol optical depth biomass burning events: A comparison of optical properties for different source regions. *Geophys. Res. Lett.* **30**: 2035, http://dx.doi.org/10.1029/2003GL017861.

Eck, T. F., B. N. Holben, A. Sinyuk, R. T. Pinker, P. Goloub, H. Chen, B. Chatenet, Z. Li, R. P. Singh, S. N. Tripathi, J. S. Reid, D. M. Giles, O. Dubovik, N. T. O'Neill, and A. Smirnov (2010), Climatological aspects of the optical properties of fine/coarse mode aerosol mixtures, J. Geophys. Res. Atmos., **115**, D19205, http://dx.doi.org/10.1029/2010JD014002.

Estevan, R., J.C. Antuña-Marrero, B. Barja, V.E. Cachorro, Á.M. de Frutos, A. Berjón, C. Toledano, B. Torres, R. Rodrígo, T.A. Hernánde, and C. E. Hernández (2011a), Preliminary results of aerosols measurements with sun photometer at Camagüey, Cuba, *Opt. Pura Appl.*, **44**(1), 99–106.

Estevan R., Y. Benouna, B. Torres, J. C. Antuña, B. Barja, C. E. Hernández, C. Toledano, D. Fuertes, R. González, V. E. Cachorro, and Á. M. de Frutos (2011b), Aerosols measurements with a CIMEL CE-318 sun photometer in Camagüey, Cuba, *Revista Boliviana de Física*, 20s, 51-53, ISSN 1562-3823.

Estevan R., L. Mona, N. Papagiannopoulos, J.C. Antuña-Marrero, V. Cachorro, Á. de Frutos (2014), CALIPSO and sun photometer measurements of Saharan dust events over Camagüey, *Opt. Pura Appl.*, **47** (3) 189-196, http://dx.doi.org/10.7149/OPA.47.3.189.

Fernández A., and Y. A. Díaz (2003), Catálogo de los Procesos Sinópticos en el Archipiélago Cubano en el período 1979-1993, *Imprenta GeoCuba*, ISBN. 959-02-0355-8, 168 pp.

Fitzgerald, E., A. P. Ault, M. Zauscher, O. L. Mayol-Bracero, and K. A. Prather (2015), Comparison of the Mixing State of Long range Transported Asian and African Mineral Dust, *Atmos. Env.*, **115**: 19–25.

García, F., R. Estevan, J. C. Antuña-Marrero1, J. Rosas, I. Y. Platero, J. C. Antuña-Sánchez., and N. Díaz, 2015, Determination of the Broadband Aerosol Optical Depth Baseline and comparison with sun photometer data. *Opt. Pura Apl.,* **48**(4), 249-58, (*In Spanish*), http://dx.doi.org/10.7149/OPA.48.4.249.

Giannini, A, Y. Kushnir, and M. A. Cane (2000), Interannual variability of Caribbean rainfall, ENSO, and the Atlantic Ocean, *J. Climate*, **13**, 297–311.

Giles, D. M., A. Sinyuk, M. G. Sorokin, J. S. Schafer, A. Smirnov, I. Slutsker, T. F. Eck, B. N. Holben, J. R. Lewis, J. R. Campbell, E. J. Welton, S. V. Korkin, and A. I. Lyapustin (2019), Advancements in the Aerosol Robotic Network (AERONET) Version 3 database – automated near-real-time quality control algorithm with improved cloud screening for Sun photometer aerosol optical depth (AOD) measurements, *Atmos. Meas. Tech.*, **12**, 169–209, https://doi.org/10.5194/amt-12-169-2019.

Gioda, A., G. J. Reyes-Rodríguez, G. Santos-Figueroa, J. L. Collet Jr., S. Decesari, M. da Conceição, K. V. Ramos, H. J. Bezerra-Netto, F. R. de Aquino-Netto, and O. L. Mayol-Bracero, (2011), Speciation of Water-soluble Inorganic, Organic, and Total Nitrogen in a Background Environment: Cloud Water, Rainwater, and Aerosol Particles, *J. Geophys. Res.*, **116**, 05203, http://dx.doi.org/10.1029/2010JD015010.

GOAC, 2020, Cooperation GOAC – GOA – UVA, (*In Spanish*), http://www.goac.cu/uva/

Goudie A.S., and N. J. Middleton (2006), Desert Dust in the Global System, *Springer Berlin Heidelberg New York*, 287pp.

Groß S., M. Tesche, V. Freudenthaler, C. Toledano, M. Weigner, A. Ansmann, D. Althausen, and M. Seefeldner (2011), Characterization of Saharan dust, marine aerosols and mixtures of biomass-burning aerosols and dust by means of multi-wavelength depolarization and Raman lidar measurements during SAMUM 2, *Tellus*, **63B**, 706–724, doi: 10.1111/j.1600-0889.2011.00556.x.

Groß S., J. Gasteiger, V. Freudenthaler, T. Müller, D Sauer, C. Toledano, and A. Ansmann (2016), Saharan dust contribution to the Caribbean rainy seasontime boundary layer – a lidar study during SALTRACE, *Atmos. Chem. Phys.*, **16**, 11535–11546, http://dx.doi.org/10.5194/acp-16-11535-2016.

Hamilton, D. S., Lee, L. A., Pringle, K. J., Reddington, C. L., Spracklen, D. V., and Carslaw, K. S (2014), Occurrence of pristine aerosol environments on a polluted planet, *P. Natl. Acad. Sci. USA*, 111, 18466–18471, doi:10.1073/pnas.1415440111, 2014.

Haywood J. M., S. R. Osborne, and S. J. Abel (2004), The effect of overlying absorbing aerosol layers on remote sensing retrievals of cloud effective radius and cloud optical depth, *Q. J. Roy. Meteor. Soc.*, 130, 779–800, doi:10.1256/qj.03.100, 2004.

Hess, M., P. Koepke, and I. Schult (1998), Optical properties of Aerosols and Clouds: The Software Package OPAC, B*ull. American Meteorol. Soc.*, **79**, 831-844.

Holben, B. N., T. F. Eck, I. Slutsker, D. Tanre, J. P. Buis, A. Setzer, E. Vermote, J. A. Reagan, Y. J. Kaufman, T. Nakajima, F. Lavenu, F. Jankowiak, and A. Smirnov (1998), AERONET – A federated instrument network and data archive for aerosol characterization, *Remote Sens. Environ.*, **66**, 1–16.

Holben, B. N., D. Tanré, A. Smirnov, T. F. Eck, I. Slutsker, N. Abuhassan, W. W. Newcomb, J. S. Schafer, B. Chatenet, F. Lavenu, Y. J. Kaufman, J. Vande Castle, A. Setzer, B. Markham, D. Clark, R. Frouin, R. Halthore, A. Karneli, N. T. O'Neill, C. Pietras, R. T. Pinker, K. Voss,and G. Zibordi (2001), An emerging ground-based aerosol climatology: Aerosol optical depth from AERONET, *J. Geophys. Res.*, **106**(D11), 12,067–12,097, http://dx.doi.org/10.1029/2001JD900014.

Jones, C., N. Mahowald, C. Luo (2003). The Role of Easterly Waves on African Desert Dust Transport, *J. Climate*, **16**, 3617-3628.

Jury, M. R., and M. J. Santiago (2010), Composite analysis of dust impacts on African easterly waves in the Moderate Resolution Imaging Spectrometer era, *J. Geophys. Res.*, **115**, D16213, http://dx.doi.org/10.1029/2009JD013612.

Jury, M. R. (2017), Caribbean Air Chemistry and Dispersion Conditions, *Atmosphere*, **8**, 151, http://dx.doi.org/10.3390/atmos8080151.

Kalnay, E., M. Kanamitsu, R. Kistler, W. Collins, D. Deaven, L. Gandin, M. Iredell, S. Saha, G. White, J. Woollen, Y. Zhu, M. Chelliah, W. Ebisuzaki, W. Higgins, J. Janowiak, K. C. Mo, C. Ropelewski, J. Wang, A. Leetmaa, R. Reynolds, R. Jenne, and D. Joseph (1996), The NCEP/NCAR 40-year reanalysis project. *Bulletin of the American Meteorological Society* **77**: 437-471.

Kambezidis, H.D., and D.G. Kaskaoutis, (2008), Aerosol climatology over four AERONET sites: An overview, *Atmos. Env.*, **42**, 1892-1906, http://dx.doi.org/10.1016/j.atmosenv.2007.11.013.

Kampa M., and E. Castanas (2008), Human health effects of air pollution, Environmental Pollution 151 (2008) 362-367, doi:10.1016/j.envpol.2007.06.012.

Kandler, K., K. Schneiders, M. Ebert, M. Hartmann, S. Weinbruch, M. Prass, and C. Pöhlker (2018), Composition and mixing state of atmospheric aerosols determined by electron microscopy: method development and application to aged Saharan dust deposition in the Caribbean boundary layer, *Atmos. Chem. Phys.*, **18**, 13429–13455, https://doi.org/10.5194/acp-18-13429-2018.

Kaskaoutis, D. G., H. D. Kambezidis, N. Hatzianastassiou, P. G. Kosmopoulos, and K. V. S. Badarinath (2007), Aerosol climatology: on the discrimination of aerosol types over four AERONET sites, *Atmos. Chem. Phys. Discuss.*, **7**, 6357–6411.

Kaskaoutis, D. G., S. Kumar, P. R. Sinha, R. P. Singh, H. D. Kambezidis, A. Sharma Rani, K. V. S. Badarinath (2011), Extremely large anthropogenic-aerosol contribution to total aerosol load over the Bay of Bengal during dry season season, Atmos. Chem. Phys. **11**, 7097-7117, http://dx.doi.org/10.5194/acp-11-7097-2011.

Kaufman, Y. J., I. Koren, L. A. Remer, D. Rosenfeld, and Y. Rudich (2005), The effect of smoke, dust, and pollution aerosol on shallow cloud development over the Atlantic Ocean, *P. Natl. Acad. Sci. USA*, 102, 11207–11212.

Kumar, K. R., N. Kang, and Y. Yin (2017), Classification of key aerosol types and their frequency distributions based on satellite remote sensing data at an industrially polluted city in the Yangtze River Delta, China. *Int. J. Climatol*., **38**, 320-336, http://dx.doi.org/10.1002/joc.5178.

Levy R. C., S. Mattoo, L. A. Munchak, L. A. Remer, A. M. Sayer, F. Patadia, and N. C. Hsu (2013), The Collection 6 MODIS aerosol products over land and ocean, *Atmos. Meas. Tech.*, **6**, 2989-3034, http://dx.doi.org/10.5194/amt-6-2989-2013.

Lohmann, U., and J. Feichter (2005), Global indirect aerosols effects: a review, *Atmos. Chem. Pys*. **5**, 715–737.

Magaña, V., J. A. Amador, and S. Medina (1999), The midrainy season drought over Mexico and Central America, *J. Climate*, **12**, 1577–1588.

Mapes, B. E., P. Liu, and N. Buenning (2005), Indian monsoon onset and Americas midrainy season drought: out-of-equilibrium responses to smooth seasonal forcing, *J. Climate*, **18**, 1109–1115.

Maring H., D. L. Savoie, M. A. Izaguirre, and L. Custals (2003), Mineral dust aerosol size distribution change during atmospheric transport, *J. Geophys. Res.*, 108, D19, 8592, doi:10.1029/2002JD002536, 2003.

Martinez C., L. Goddard, Y. Kushnir, and M. Ting (2019), Seasonal climatology and dynamical mechanisms of rainfall in the Caribbean, Clim. Dyn., **53,** 825–846, https://doi.org/10.1007/s00382-019-04616-4.

Middleton N. J., and A. S. Goudie (2001), Saharan dust: sources and trajectories, *Transactions of the Institute of British Geographers, New Series*, Vol. 26, No. 2 (2001).

Michelangeli, P.A., R. Vautard, and B. Legras (1995), Weather Regimes: Recurrence and Quasi Stationarity. *J. Atmos. Sci*. 52, 1237–1256. doi: 10.1175/1520-0469(1995)052<1237:WRRAQS>2.0.CO;2.

Monteil M. A. (2008), Saharan dust clouds and human health in the English-speaking Caribbean: what we know and don't know, *Environ. Geochem. Health* (2008) 30:339–343, doi: 10.1007/s10653-008-9162-0.

Moron, V., I. Gouirand, and M. Taylor (2016), Weather types across the Caribbean basin and their relationship with rainfall and sea surface temperature. *Clim. Dyn.*, 47**,** 601–621. DOI 10.1007/s00382-015-2858-9.

MVO Activity Reports 2010, Open File Report OFR 13-03 (March 2013), Montserrat Volcano Observatory - P.O. Box 318 - Flemmings – Montserrat, http://www.mvo.ms/pub/Activity_Reports/2010/MVO_OFR_13_03-MVO_Activity_Reports_2010.pdf

MVO Activity Reports 2012, Open File Report OFR 13-01 (January 2013), Montserrat Volcano Observatory - P.O. Box 318 - Flemmings – Montserrat, http://www.mvo.ms/pub/Activity_Reports/2012/MVO_OFR_13_01-MVO_Activity_Reports_2012.pdf

MVO Activity Reports 2013, Open File Report OFR 14-01 (January 2014), Montserrat Volcano Observatory - P.O. Box 318 - Flemmings – Montserrat, http://www.mvo.ms/pub/Open_File_Reports/MVO_OFR_14_01-MVO_Activity_Reports_2013.pdf

Myhre, G., D. Shindell, F.-M. Bréon, W. Collins, J. Fuglestvedt, J. Huang, D. Koch, J.-F. Lamarque, D. Lee, B. Mendoza, T. Nakajima, A. Robock, G. Stephens, T. Takemura and H. Zhang (2013), Anthropogenic and Natural Radiative Forcing. In: Climate Change 2013: The Physical Science Basis. Contribution of Working Group I to the Fifth Assessment Report of the Intergovernmental Panel on Climate Change [Stocker, T.F., D. Qin, G.-K. Plattner, M. Tignor, S.K. Allen, J. Boschung, A. Nauels, Y. Xia, V. Bex and P.M. Midgley (eds.)]. *Cambridge University Press*, Cambridge, United Kingdom and New York, NY, USA.

New N., and J. Estupiñán (2013), Meteorological Condition leading to the Saharan events observed in South Florida in July 2012, An internship report for the Master of Professional Science Program, *Rosenstiel School of Marine and Atmospheric Science, University of Miami, in cooperation with The National Weather Service Miami Forecast Office.*

O'Neill, N.T., A. Ignatov, B. N. Holben, T. F. Eck (2000), The lognormal distribution as a reference for reporting aerosol optical depth statistics; empirical tests using multi-year, multi-site AERONET sun photometer data, *Geophys. Res. Lett.,* **27**, 3333–3336.

O’Neill, N.T., T. F. Eck, B. N. Holben, A. Smirnov, A. Royer, Z. Li (2002), Optical properties of boreal forest fire smoke derived from Sun photometry. *J. Geophys. Res.* **107**(D11): https://doi.org/10.1029/2001JD000877.

Patel P.N., U.C. Dumka, D.G. Kaskaoutis, K.N. Babu, Alok K. Mathur (2017), Optical and radiative properties of aerosols over Desalpar, a remote site in western India: Source identification, modification processes and aerosol type discrimination, *Sci. Tot. Env.* 575 (2017) 612–627, http://dx.doi.org/10.1016/j.scitotenv.2016.09.023.

Petit, R. H., M. Legrand, I. Jankowiak, J. Molinié, C. Asselin de Beauville, G. Marion, and J. L. Mansot (2005), Transport of Saharan dust over the Caribbean Islands: Study of an event, J. Geophys. Res., 110, D18S09, doi:10.1029/2004JD004748.

Prospero, J. M., E. Bonatti, C. Schubert, and T. N. Carlson (1970), Dust in the Caribbean atmosphere traced to an African dust storm, *Earth Planet. Sci. Lett.*, **9**, 287–293.

Prospero, J. and T. Carlson (1972): Vertical and areal distribution of Saharan dust over the western equatorial North Atlantic Ocean, *J. Geophys. Res.*, **77**, 5255–5265, http://dx.doi.org/10.1029/JC077i027p05255.

Prospero, J. M., & Nees, R. T. (1986). Impact of the North African drought and El Niño on mineral dust in the Barbados trade winds. *Nature,* 320, 735. https://doi.org/10.1038/320735a0.

Prospero, J. M., F.-X. Collard, J. Molinié, and A. Jeannot (2014), Characterizing the annual cycle of African dust transport to the Caribbean Basin and South America and its impact on the environment and air quality, *Global Biogeochem. Cycles*, **29**, 757–773, http://dx.doi.org/10.1002/2013GB004802.

Prospero, J. M., and H. F. Diaz (2016), The impact of African dust on air quality in the Caribbean Basin, *Eos*, **97**, http://dx.doi.org/10.1029/2016EO043831.

Raga, G. B., D. Baumgardner, and O. L. Mayol-Bracero (2016), History of Aerosol-Cloud Interactions Derived from Observations in Mountaintop Clouds in Puerto Rico. *Aerosol Air Qual. Res.*, **16**, 674-688, http://dx.doi.org/10.4209/aaqr.2015.05.0359.

Raptis I.P., S. Kazadzis , V. Amiridis , A. Gkikas, E. Gerasopoulos, and N. Mihalopoulos (2020), A Decade of Aerosol Optical Properties Measurements over Athens, Greece, *Atmosphere*,, **11**, 154; http://dx.doi.org/10.3390/atmos11020154.

Reddington, C. L., and Coauthors, (2017), The Global Aerosol Synthesis and Science Project (GASSP): Measurements and Modeling to Reduce Uncertainty. *Bull. Amer. Meteor. Soc.*, **98**, 1857–1877, https://doi.org/10.1175/BAMS-D-15-00317.1.

Rittmeister F., A. Ansmann, R. Engelmann, A. Skupin, H. Baars, T. Kanitz, and S. Kinne (2017), From the Caribbean toWest Africa: Four weeks of continuous dust and marine aerosol profiling with shipborne polarization/Raman lidar— a contribution to SALTRACE, *Atmos. Chem. Phys. Discuss.*, doi:10.5194/acp-2017-130, 2017.

Rivera, H., J. A. Ogren, E. Andrews, O. L. Mayol-Bracero (2018), Variations in the physicochemical and optical properties of natural aerosols in Puerto Rico - Implications for climate, *Atmos. Chem. Phys. Discuss.*, https://doi.org/10.5194/acp-2018-791.

Roberts, G. C., and A. Nenes (2005), A Continuous-Flow Streamwise Thermal-Gradient CCN Chamber for Atmospheric Measurements, *Aerosol Science and Technology*, **39**, 206-221, http://dx.doi.org/10.1080/027868290913988.

Sáenz, F. and A. M. Durán-Quesada (2015), A climatology of low level wind regimes over Central America using a weather type classification approach, *Front. Earth Sci.*, **3**, 15, http://dx.doi.org/10.3389/feart.2015.00015.

Sears, T. M., G. E. Thomas, E. Carboni, A. J. A. Smith, and R. G. Grainger (2013), SO^2 as a possible proxy for volcanic ash in aviation hazard avoidance, *J. Geophys. Res. Atmos.*, **118**, 5698–5709, https://doi.org/10.1002/jgrd.50505.

Sellitto P., L. Spampinato, G. G. Salerno, and A. La Spina (2018), Aerosol Optical Properties of Pacaya Volcano Plume Measured with a Portable Sun photometer, *Geosciences*, **8**, 36; https://doi.org/10.3390/geosciences8020036.

Schultz, D.M., W.E. Bracken, and L.F. Bosart (1998), Planetary- and synoptic-scale signatures associated with Central American Cold Surges. *Mon. Wea.Rev*. 126, 5–27. doi: 10.1175/1520-0493(1998)126<0005: PASSSA>2.0.CO;2

Smirnov, A., B. N. Holben, T. F. Eck, O. Dubovik, and I. Slutsker (2000), Cloud screening and quality control algorithms for the AERONET data base, *Remote Sens. Env.*, **73**, 337–349.

Smirnov, A., B. N. Holben, Y, J. Kaufman, O. Dubovik, T. F. Eck, I. Slutsker, C. Pietras, and R. Halthore (2002), Optical properties of atmospheric aerosol in maritime environments, *J. Atmos. Sci.,* **59**, 501–523.

Snider, J., M. Petters, P. Wechsler, and P. Liu, 2006: Supersaturation in the Wyoming CCN Instrument. *Journal of Atmospheric and Oceanic Technology*, **23**, 1323–1339.

Spiegel, J. K., N. Buchmann, O. L. Mayol-Bracero, L. A. Cuadra-Rodríguez, C. J. Valle-Díaz, K. A. Prather, S. Mertes and W. Eugster (2013), Do Cloud Properties in a Puerto Rican Tropical Montane Cloud Forest Depend on Occurrence of Long range Transported African Dust?, *Pure Appl. Geophys.*, **171**, 2443–2459.

Taylor M.A, and E.J. Alfaro (2005), Central America and the Caribbean, Climate of. In: Oliver JE (ed) Encyclopedia of world climatology. Encyclopedia of earth sciences series. *Springer*, Dordrecht, https://doi.org/10.1007/1-4020-3266-8.

Tesche, M., S. Groß, A. Ansmann, D. Müller, D. Althausen, V. Freudenthaler, and M. Esselborn (2011), Profiling of Saharan dust and biomass burning smoke with multiwavelength polarization Raman lidar at Cape Verde. *Tellus* **63B**, 649–676, doi: 10.1111/j.1600-0889.2011.00548.x.

Toledano, C. (2005), Climatología de los aerosoles mediante la caracterización de propiedades ópticas y masas de aire en la estación 'El Arenosillo' de la red AERONET, Tesis presentada para optar por el grado de Doctor en Ciencias. Universidad de Valladolid. 237 pp.

Toledano, C., V. E. Cachorro, A. Berjon, A. M. de Frutos, M. Sorribas, B. A. de la Morena, and P. Goloub (2007), Aerosol optical depth and Ångström Exponent climatology at El Arenosillo AERONET site (Huelva, Spain), *Q. J. R. Meteorol. Soc.*, **133**, 795-807, http://dx.doi.org/10.1002/qj.54.

Toledano, C., V. E. Cachorro, A. M. de Frutos, B. Torres, A. Berjón, M. Sorribas, and S. Stone (2009), Airmass Classification and Analysis of Aerosol Types at El Arenosillo (Spain), *J. Appl. Met. Clim.*, **48**, 962-981, http://dx.doi.org/10.1175/2008JAMC2006.1

Valle-Díaz, C. J., E. Torres-Delgado, S. M. Colón-Santos, T. Lee, J. L. Collett Jr., W. H. McDowell, and O. M. Mayol-Bracero (2016), Impact of long-range transported African dust on cloud water chemistry at a tropical montane cloud forest in northeastern Puerto Rico, *Aerosol and Air Quality Research.*, **16**, 653-664, http://dx.doi.org/10.4209/aaqr.2015.05.0320.

Velasco-Merino, C., D. Mateos, C. Toledano, J. M. Prospero, J. Molinie, L. Euphrasie-Clotilde, R. González, V. E. Cachorro, A. Calle, and A. M. de Frutos (2018), Impact of long-range transport over the Atlantic Ocean on Saharan dust optical and microphysical properties based on AERONET data, *Atmos. Chem. Phys.*, **18**, 9411-9424, https://doi.org/10.5194/acp-18-9411-2018.

Verma, S., D. Prakash, P. Ricaud, S. Payra, J. L. Attié, M. Soni (2015), A New Classification of Aerosol Sources and Types as Measured over Jaipur, India, *Aerosol and Air Quality Research*, **15**, 985–993.

Weigel, R., S. Borrmann, J. Kazil, A. Minikin, A. Stohl, J. C. Wilson, J. M. Reeves, D. Kunkel, M. de Reus, W. Frey, E. R. Lovejoy, C. M. Volk, S. Viciani, F. D'Amato, C. Schiller, T. Peter, H. Schlager, F. Cairo, K. S. Law, G. N. Shur, G. V. Belyaev, and J. Curtius (2011), In situ observations of new particle formation in the tropical upper troposphere: the role of clouds and the nucleation mechanism, *Atmos. Chem. Phys.*, **11**, 9983–10010, http://dx.doi.org/10.5194/acp-11-9983-2011

Weinzierl B., A. Ansmann, J. M. Prospero, D. Althausen, N. Benker, F. Chouza, M. Dollner, D. Farrell, W. K. Fomba, V. Freudenthaler, J. Gasteiger, S. Groß, M. Haarig, B. Heinold, K. Kandler, T. B. Kristensen, O. L. Mayol-Bracero, T. Müller, O. Reitebuch, D. Sauer, A. Schäfler, K. Schepanski, A. Spanu, I. Tegen, C. Toledano, and A. Walser (2017), The Saharan Aerosol Long-Range Transport and Aerosol-Cloud-Interaction Experiment, *Bull. Amer. Meteor. Soc.*, **98**, 1427-1451, http://dx.doi.org/10.1175/BAMS-D-15-00142.1.

Wex, H., K. Dieckmann, G. C. Roberts, T. Conrath, M. A. Izaguirre, S. Hartmann, P. Herenz, M. Schäfer, F. Ditas, T. Schmeissner, S. Henning, B. Wehner, H. Siebert, and F. Stratmann (2016), Aerosol arriving on the Caribbean island of Barbados:

physical properties and origin, *Atmos. Chem. Phys.*, **16**, 14107–14130, http://dx.doi.org/10.5194/acp-16-14107-2016.

Xian P., P. J. Klotzbach, J. P. Dunion, M. A. Janiga, J. S. Reid, P. R. Colarco, and Z. Kipling (2020), Revisiting the Relationship between Atlantic Dust and Tropical Cyclone Activity using Aerosol Optical Depth Reanalyses: 2003-2018, *Atmos. Chem. Phys.* Preprint. Discussion started: 15 June 2020, https://doi.org/10.5194/acp-2020-287.

Zhang, R. J., K. F. Ho and Z. X. Shen (2012), The Role of Aerosol in Climate Change, the Environment, and Human Health, *Atmospheric and Oceanic Science Letters*, **5**, 2, 156-161, http://dx.doi.org/10.1080/16742834.2012.11446983.

Zhao B., J. H. Jiang, D. J. Diner, H. Su, Y. Gu, K.N. Liou, Z. Jiang, L. Huang, Y. Takano, X. Fan, and A. H. Omar (2018), Intra-annual variations of regional aerosol optical depth, vertical distribution, and particle types from multiple satellite and ground-based observational datasets, *Atmos. Chem. Phys.*, 18, 11247–11260, https://doi.org/10.5194/acp-18-11247-2018.

Table captions

Table 1. Characteristics of the Caribbean AERONET stations used in this study. The last but one column shows the number of non-missing days for the Level 2.0 of the AERONET Version 3.0 dataset over the analyzed period 7 October 2008 - 31 December 2016.

Table 2. Climatology (annual mean and interannual standard deviation, 2008-2016) of daily mean AOD_{440} and $AE_{440-870}$ for each Caribbean station.

Table 3. Thresholds of daily mean AOD_{440} and $AE_{440-870}$ values used for the aerosol type classification.

Table 4. Total number of days per aerosol type at each station in the analyzed period. The relative frequencies (in percentage of days) are shown in parentheses.

Figure captions

Figure 1. Map of the Caribbean AERONET stations used in this study and Zones of air masses (source regions) associated with aerosol transport to the Caribbean region.

Figure 2. Climatological (2008-2016) mean annual cycle of AOD_{440} (dimensionless) for each Caribbean station. Gray shading shows the monthly mean plus / minus one (interannual) standard deviation. The whiskers denote 1.5 times the interquartile range and the boxes indicate the 25^{th} and 75^{th} percentiles, with the median in between.

Figure 3. Total frequency distribution of daily mean $\ln AOD_{440}$ over the analyzed period for each Caribbean station. Thick lines represent the multi-mode normal fits of the distribution, with thin lines denoting the underlying normal distributions obtained from the Gaussian mixture model (see text for details).

Figure 4. As Figure 2 but for $AE_{440-870}$ (dimensionless).

Figure 5. As Figure 3 but for $AE_{440-870}$.

Figure 6. Scatter plot of AOD_{440} vs $AE_{440-870}$ based on daily mean data at each station. The color scale indicates the density of measurements using bins of 0.01 for AOD_{440} and $AE_{440-870}$. The regions delimiting the type of aerosol in the AOD_{440} - $AE_{440-870}$ space are highlighted.

Figure 7. Monthly frequency distribution (in percentage of days in the month) of aerosol types for each Caribbean station. The number above the bars indicates the total frequency of days in that month over the analyzed period.

Figure 8. Composites (2008-2016) of geopotential height (shading, m) and wind vector (arrows) anomalies at 850 hPa for the dry season days classified in each weather type. The top right of each panel shows the percentage of seasonal days with each weather type.

Figure 9. As Figure 8 but for the rainy season.

Figure 10. Change in the probability of occurrence of weather types (columns) for the days with different aerosol types (rows) at each Caribbean station (panels): a) dry season; b) rainy season. Probability changes are expressed with respect to the climatology, using all days of the corresponding season. The sign (*) denotes statistical significance at $p<0.01$ or $p>0.99$ according to a binomial test. Hatched (grey) cells identify aerosol types with less than 20% of occurrence (no episodes) in the given season.

Figure 11. Composites of geopotential height (shading, m) and wind vector (arrows) anomalies at 850 hPa for the first day of marine aerosol episodes in the dry season and each Caribbean station. Contours show the mean geopotential height at 850 hPa for the composited days (m). The three colored lines indicate the mean backward trajectories arriving at 500 m (green), 1500 m (magenta) and 3000 m (brown), with colored dots denoting the mean positions for each day of the 7-day backward trajectories. The top right of each panel shows the number of cases employed in the composite with respect to the total number of days with that aerosol. See text for details.

Figure 12. As Figure 11 but for the dust aerosol episodes in the rainy season. White dots indicate significant differences in geopotential height with respect to the climatology at the 90% confidence level, as derived from a 1000-trial Monte Carlo test.

Figure 13. Main source regions of aerosol type episodes (rows) at the Caribbean stations (columns) for the: a) dry and b) rainy season. For each station the left / middle / right columns show the main sources of the backward trajectories initialized at 500 / 1500 / 3000 m. Colors identify the source region according to the legend, with the degree of darkness denoting the level of contribution (light / medium / dark shading corresponds to <40, [40-55], >55% of episodes in the season). Hatched (grey) cells

identify aerosol types with less than 20% of occurrence (no episodes) in the given season.

Figure A1. Classifiability index CI distribution against the number of clusters. The black line shows the observed CI. The red solid line is the one-sided $p<0.01$ significance level from 100 red-noise simulations.

Table 1. Characteristics of the Caribbean AERONET stations used in this study. The last but one column shows the number of non-missing days for the Level 2.0 of the AERONET Version 3.0 dataset over the analyzed period 7 October 2008 - 31 December 2016.

Station	Lat, Lon (N,E)	Elevation (m)	Size of the island (km^2)	Distance to the sea (km)	Distance to North America (km)	Start date of available measurements	Non-missing days in the analyzed period	Cloud free days (% of non-missing days)
Ragged Point (Barbados)	13.17, -59.43	40.0	432 km^2	0.052	2715	28/8/2007	1556	67
Guadeloupe (Overseas territory of France)	16.22, -61.53	39.0	848 km^2	0.385	2275	18/2/1997	1197	66
La Parguera (Puerto Rico)	17.97, -67.05	12.4	8900 km^2	0.095	1790	30/6/2000	1804	85
Camagüey (Cuba)	21.42, -77.85	122.0	109884 km^2	85	578	7/10/2008	1497	78

Table 2. Climatology (annual mean and interannual standard deviation, 2008-2016) of daily mean AOD_{440} and $AE_{440-870}$ for each Caribbean station.

	Ragged Point	Guadeloupe	La Parguera	Camagüey
AOD_{440}	0.16 ± 0.12	0.16 ± 0.14	0.15 ± 0.12	0.16 ± 0.09
$AE_{440-870}$	0.28 ± 0.22	0.33 ± 0.31	0.50 ± 0.34	0.88 ± 0.42

Table 3. Thresholds of daily mean AOD_{440} and $AE_{440\text{-}870}$ values used for the aerosol type classification.

Aerosol Type	Classification criteria
Marine	$AOD \leq 0.18$ and $AE \leq 1.05$
Continental	$AOD \leq 0.18$ and $AE > 1.05$
Pure Dust	$AOD > 0.18$ and $AE \leq 0.7$
Mixture Dust	$AOD > 0.18$ and $0.7 < AE \leq 1.5$
Polluted	$0.18 < AOD \leq 0.35$ and $AE > 1.5$
Biomass Burning	$AOD > 0.35$ and $AE \geq 1.5$

Table 4. Total number of days per aerosol type at each station in the analyzed period. The relative frequencies (in percentage of days) are shown in parentheses.

Aerosol Type	Stations			
	Ragged Point	Guadeloupe	La Parguera	Camagüey
Marine	1085 (69.7%)	820 (68.5%)	1271 (70.4%)	715 (47.7%)
Continental	12 (0.8%)	53 (4.4%)	99 (5.5%)	304 (20.3%)
Pure Dust	453 (29.1%)	319 (26.7%)	375 (20.8%)	130 (8.7%)
Mixture Dust	6 (0.4%)	5 (0.4%)	54 (3.0%)	280 (18.7%)
Polluted	0 (0%)	0 (0%)	4 (0.2%)	57 (3.8%)
Biomass Burning	0 (0%)	0 (0%)	1 (~0%)	11 (0.7%)

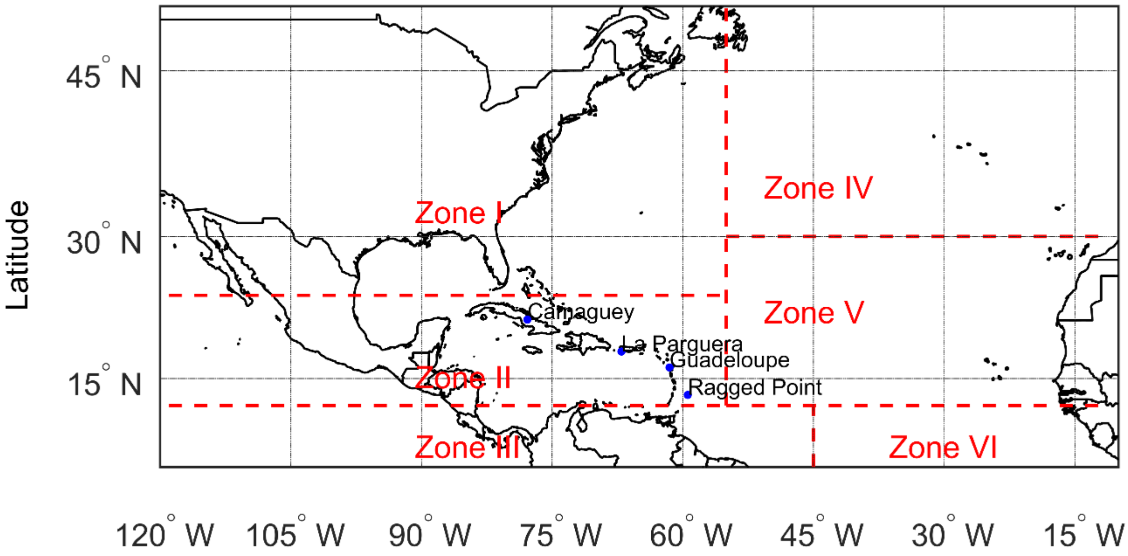

Figure 1. Map of the Caribbean AERONET stations used in this study and Zones of air masses (source regions) associated with aerosol transport to the Caribbean region.

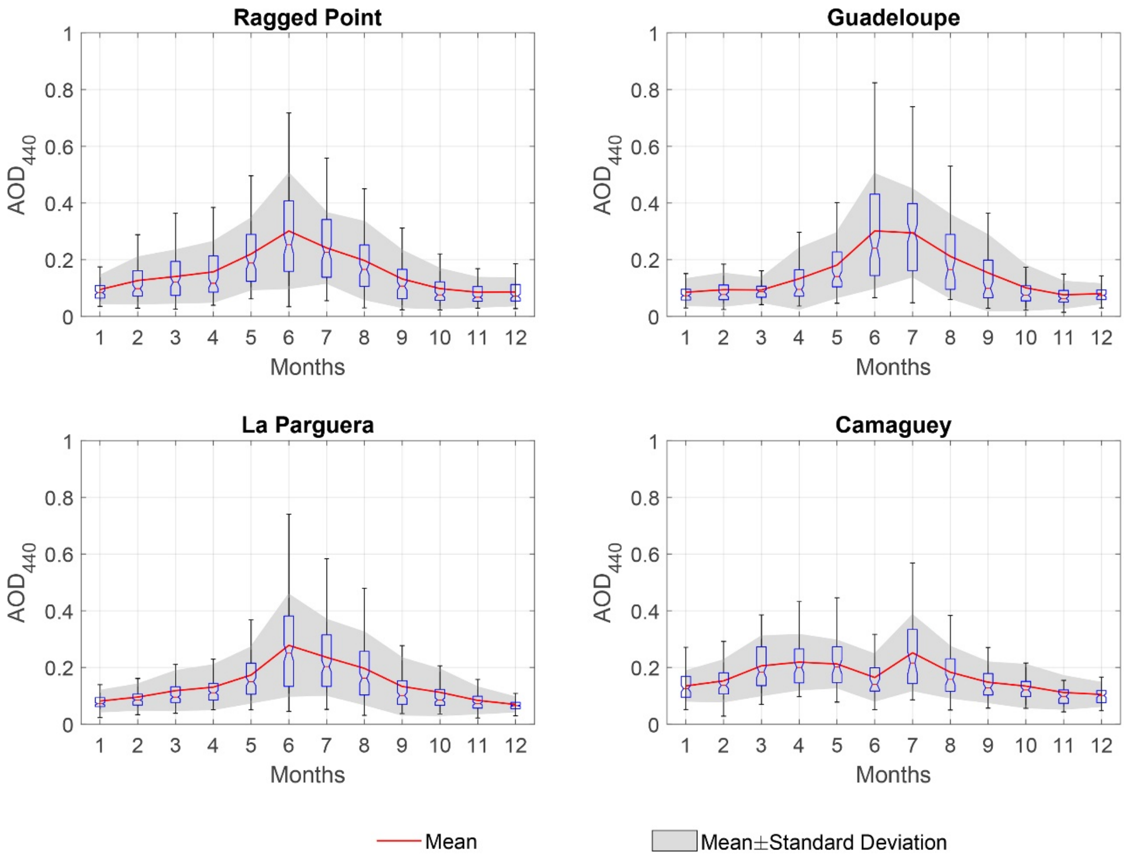

Figure 2. Climatological (2008-2016) mean annual cycle of AOD_{440} (dimensionless) for each Caribbean station. Gray shading shows the monthly mean plus / minus one (interannual) standard deviation. The whiskers denote 1.5 times the interquartile range and the boxes indicate the 25^{th} and 75^{th} percentiles, with the median in between.

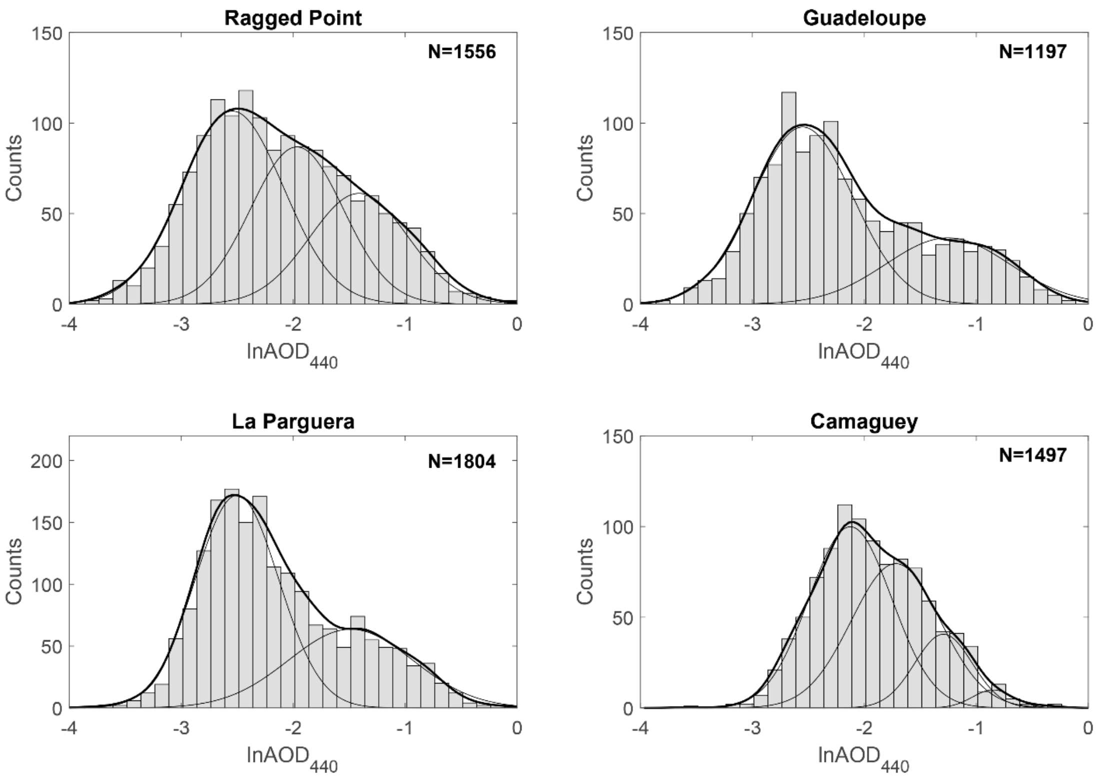

Figure 3. Total frequency distribution of daily mean $lnAOD_{440}$ over the analyzed period for each Caribbean station. Thick lines represent the multi-mode normal fits of the distribution, with thin lines denoting the underlying normal distributions obtained from the Gaussian mixture model (see text for details).

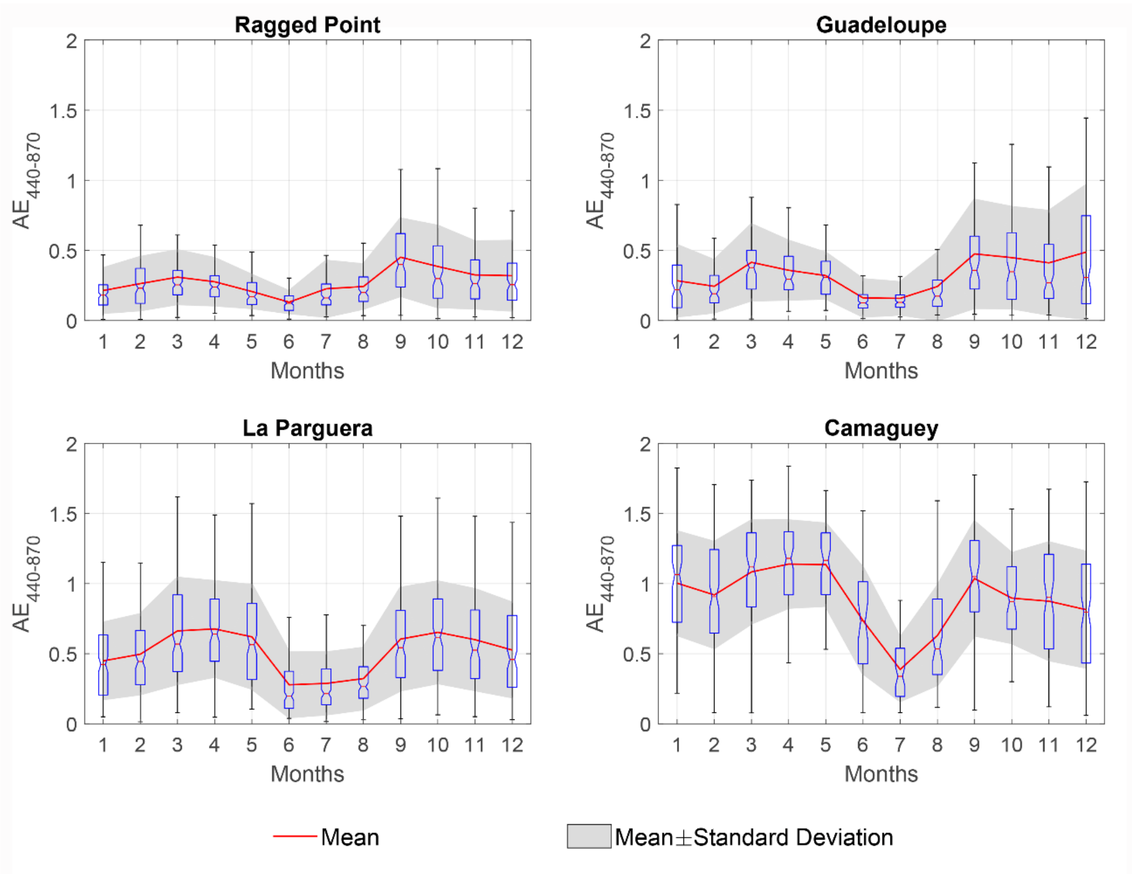

Figure 4. As Figure 2 but for $AE_{440-870}$ (dimensionless).

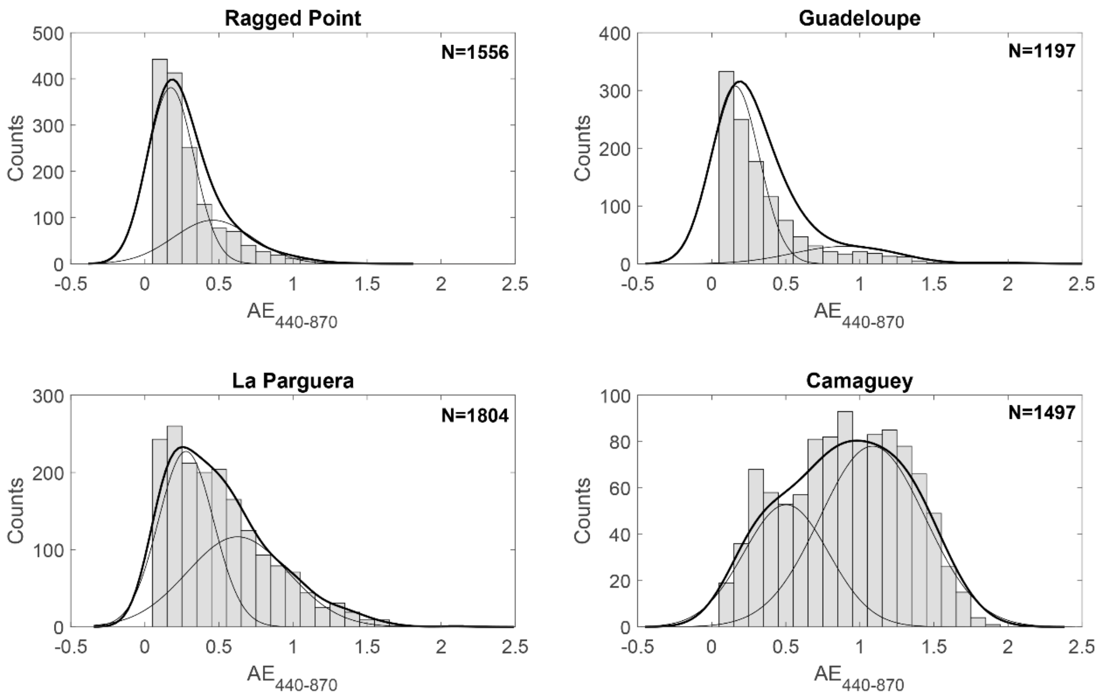

Figure 5. As Figure 3 but for $AE_{440-870}$.

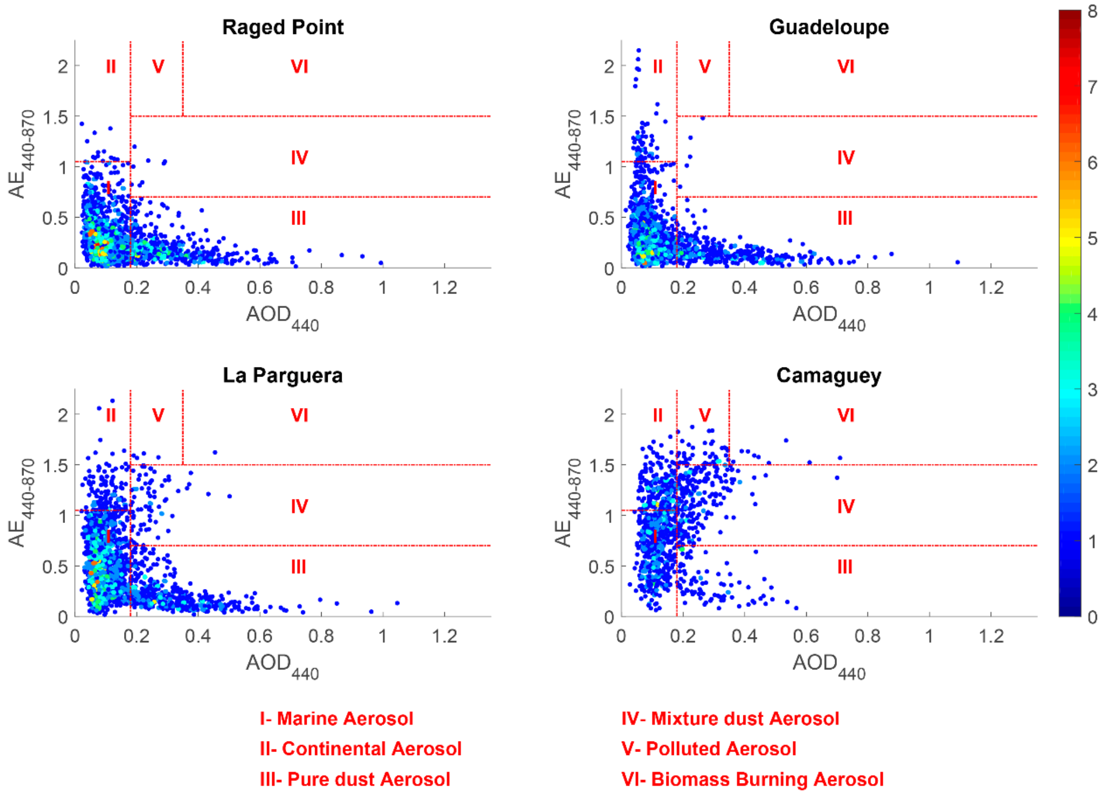

Figure 6. Scatter plot of AOD_{440} vs $AE_{440-870}$ based on daily mean data at each station. The color scale indicates the density of measurements using bins of 0.01 for AOD_{440} and $AE_{440-870}$. The regions delimiting the type of aerosol in the AOD_{440} - $AE_{440-870}$ space are highlighted.

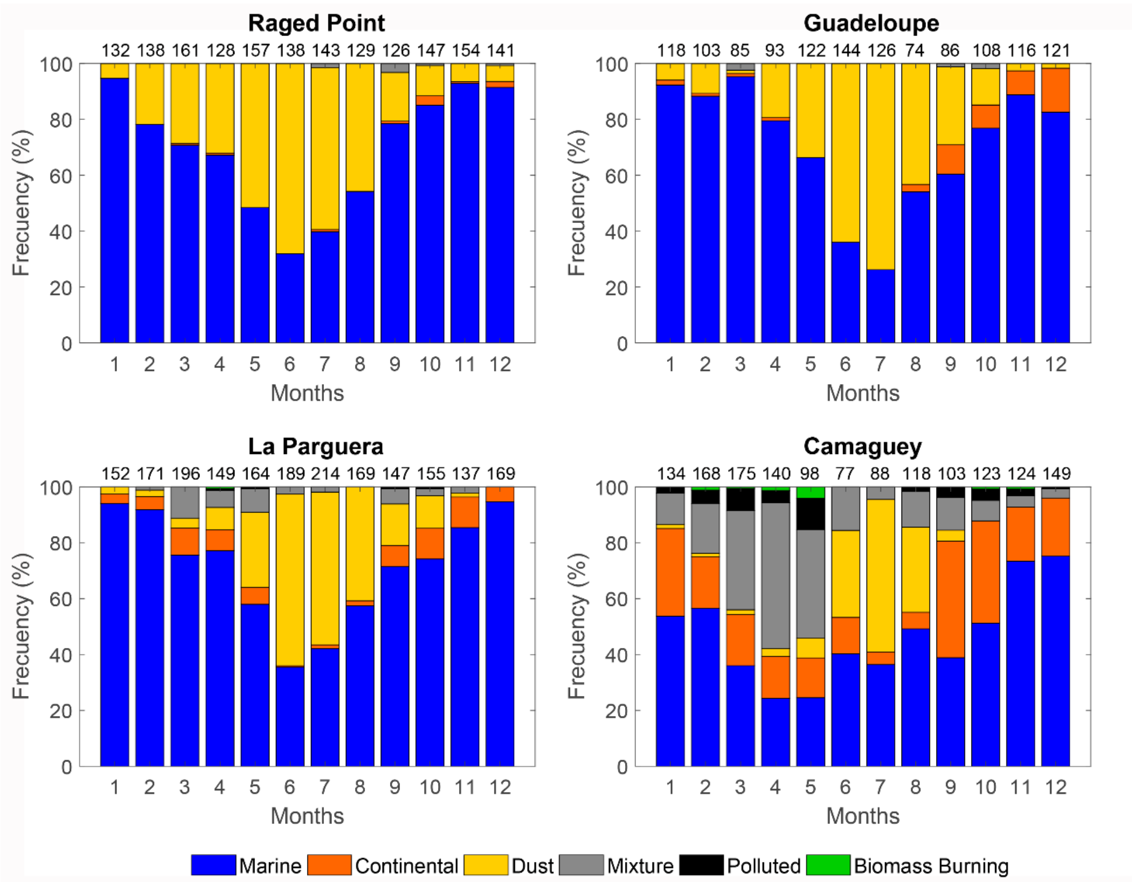

Figure 7. Monthly frequency distribution (in percentage of days in the month) of aerosol types for each Caribbean station. The number above the bars indicates the total frequency of days in that month over the analyzed period.

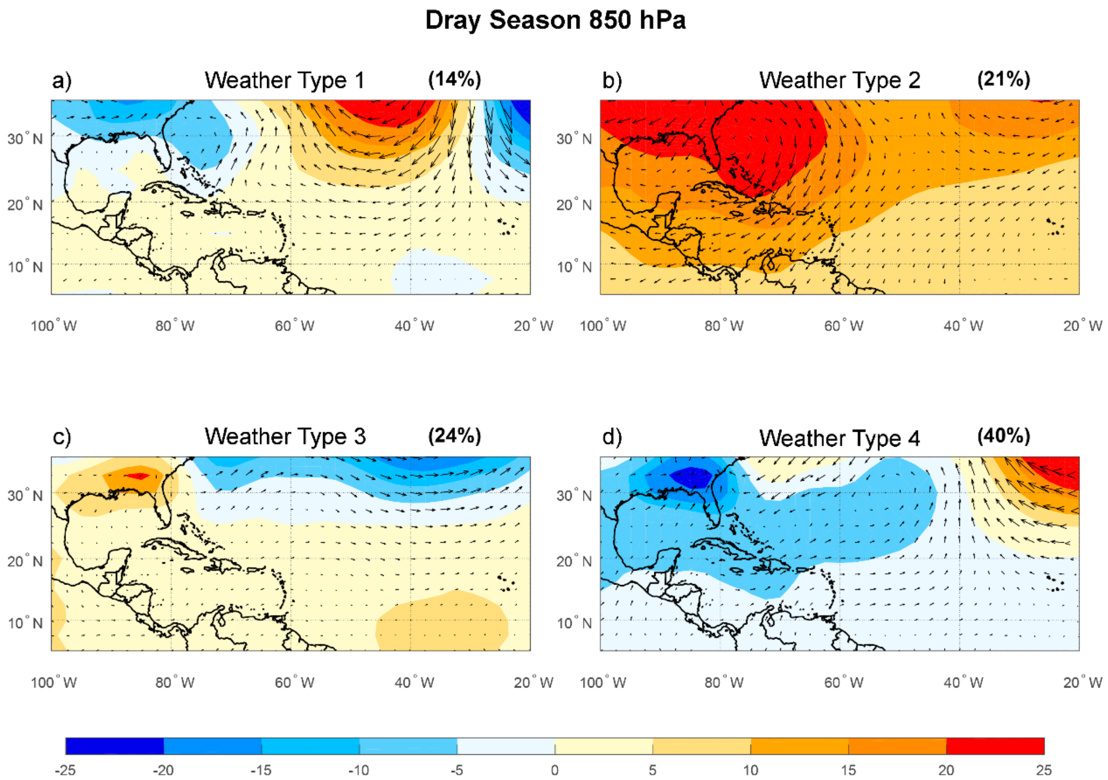

Figure 8. Composites (2008-2016) of geopotential height (shading, m) and wind vector (arrows) anomalies at 850 hPa for the dry season days classified in each weather type. The top right of each panel shows the percentage of seasonal days with each weather type.

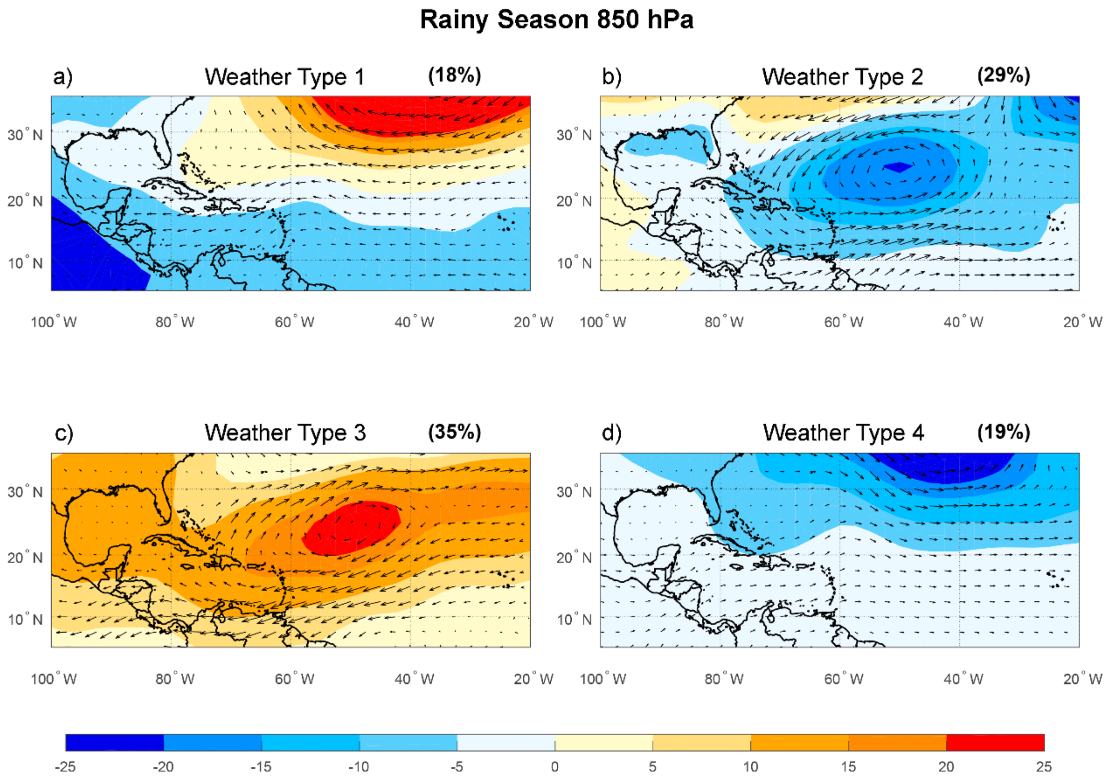

Figure 9. As Figure 8 but for the rainy season.

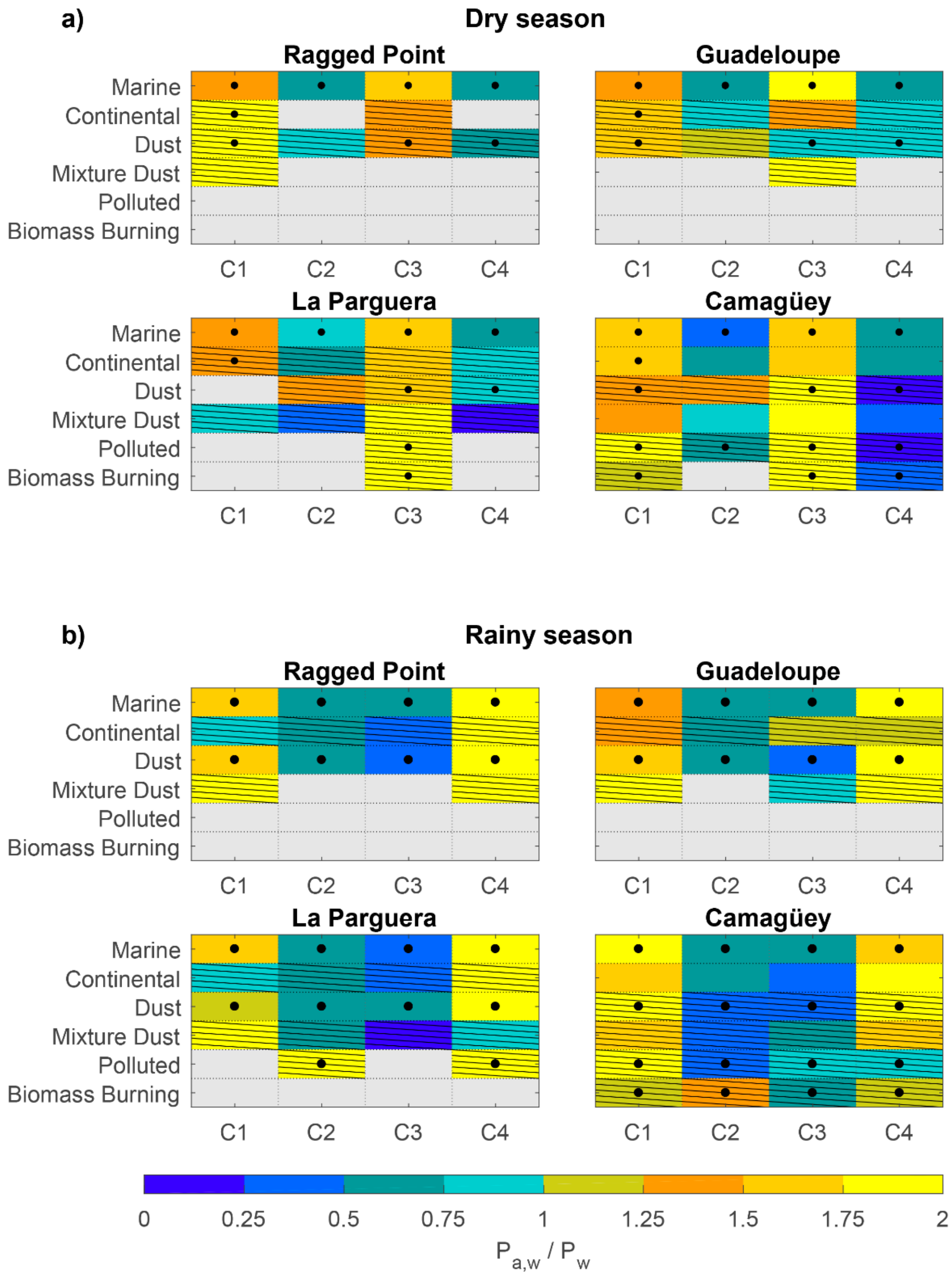

Figure 10. Change in the probability of occurrence of weather types (columns) for the days with different aerosol types (rows) at each Caribbean station (panels): a) dry season; b) rainy season. Probability changes are expressed with respect to the climatology, using all days of the corresponding season. The sign (*) denotes statistical significance at p<0.01 or p>0.99 according to a binomial test. Hatched (grey) cells identify aerosol types with less than 20% of occurrence (no episodes) in the given season.

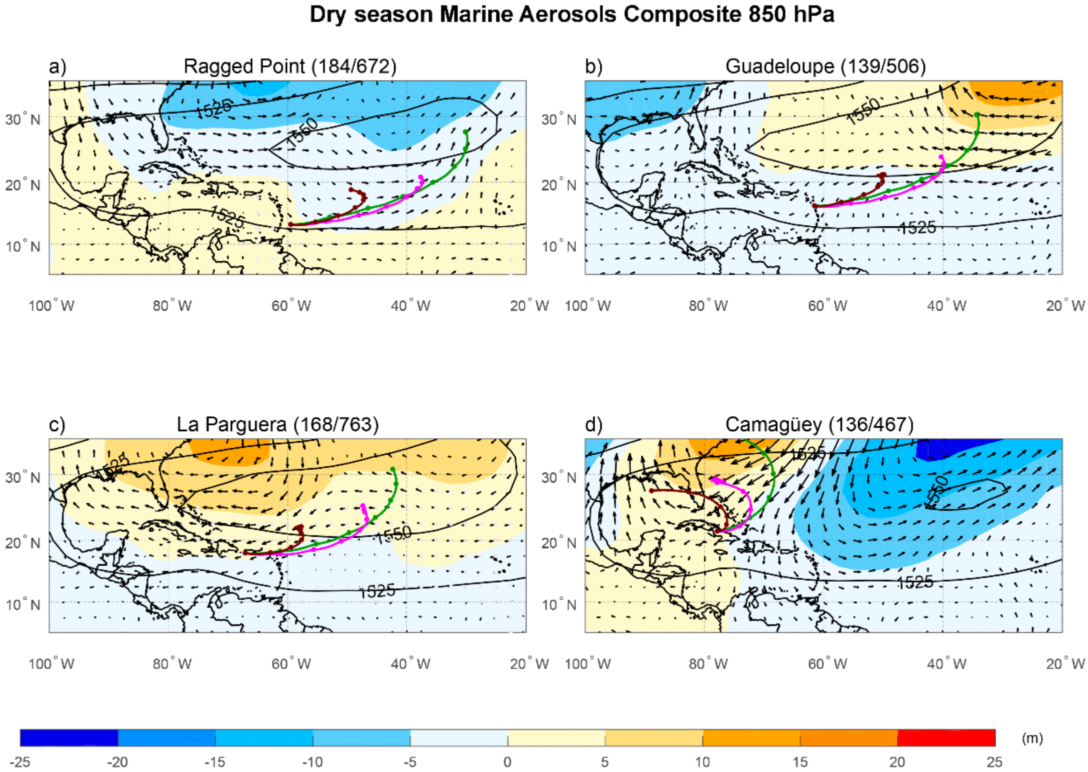

Figure 11. Composites of geopotential height (shading, m) and wind vector (arrows) anomalies at 850 hPa for the first day of marine aerosol episodes in the dry season and each Caribbean station. Contours show the mean geopotential height at 850 hPa for the composited days (m). The three colored lines indicate the mean backward trajectories arriving at 500 m (green), 1500 m (magenta) and 3000 m (brown), with colored dots denoting the mean positions for each day of the 7-day backward trajectories. The top right of each panel shows the number of cases employed in the composite with respect to the total number of days with that aerosol. See text for details.

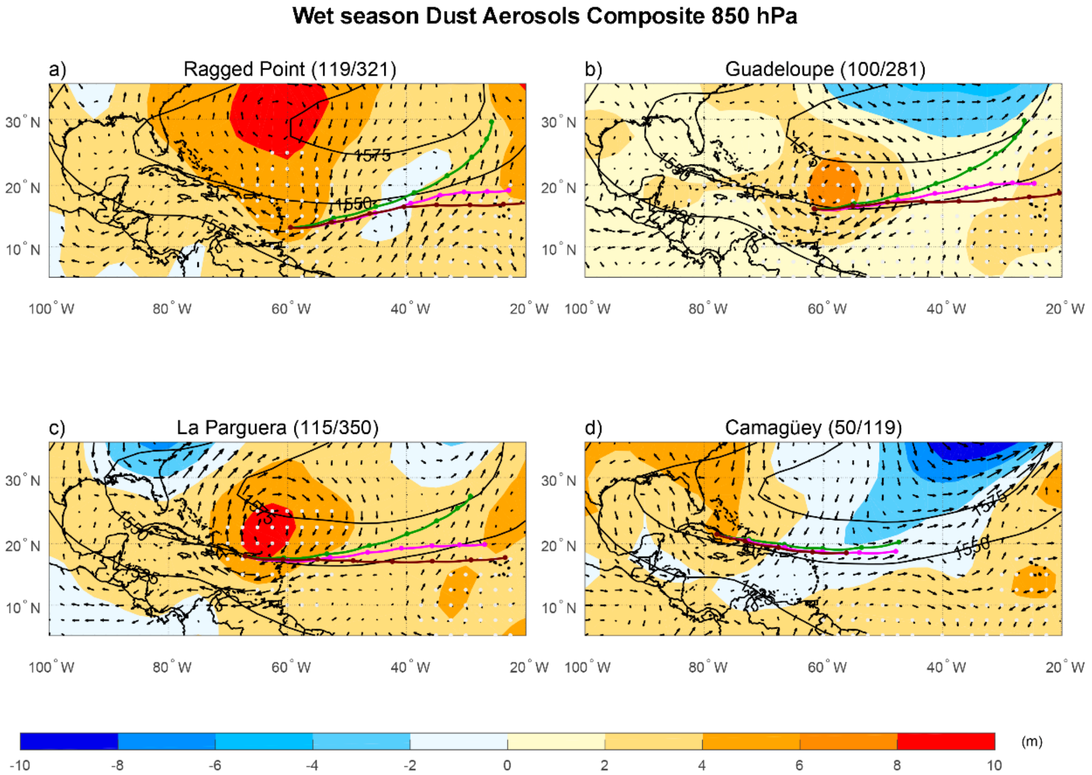

Figure 12. As Figure 11 but for the dust aerosol episodes in the rainy season. White dots indicate significant differences in geopotential height with respect to the climatology at the 90% confidence level, as derived from a 1000-trial Monte Carlo test.

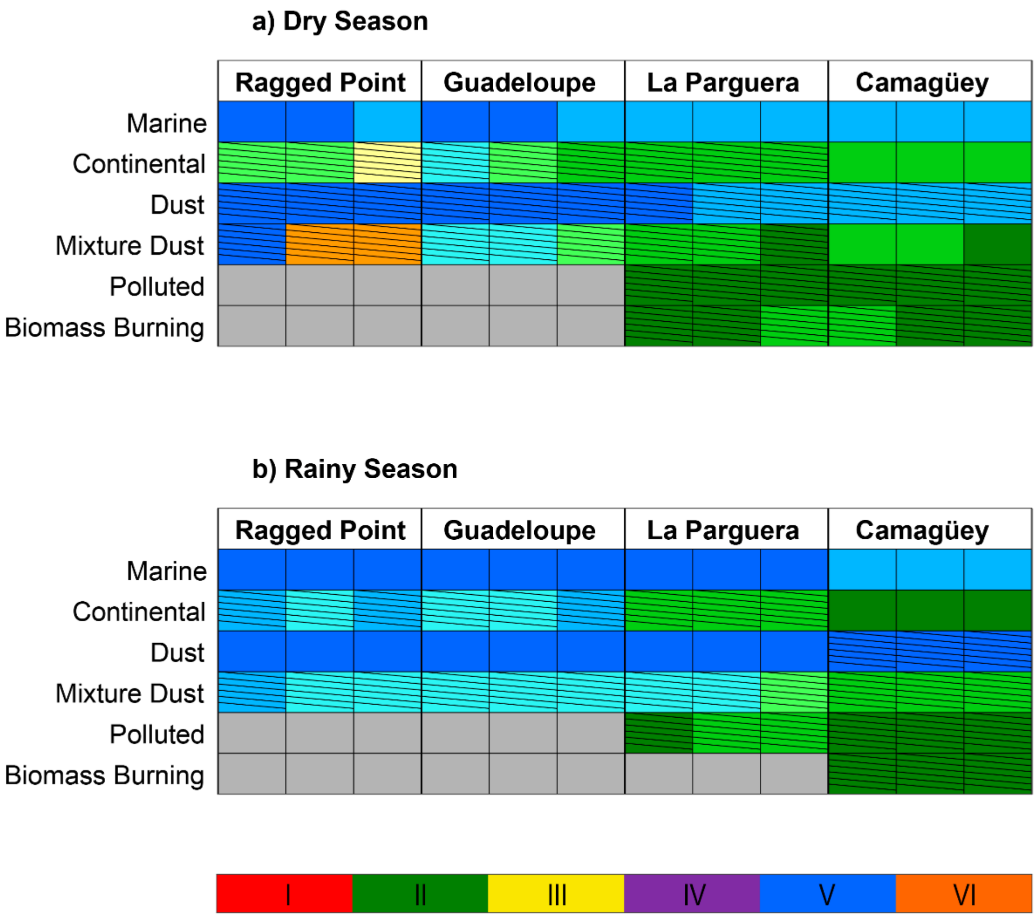

Figure 13. Main source regions of aerosol type episodes (rows) at the Caribbean stations (columns) for the: a) dry and b) rainy season. For each station the left / middle / right columns show the main sources of the backward trajectories initialized at 500 / 1500 / 3000 m. Colors identify the source region according to the legend, with the degree of darkness denoting the level of contribution (light / medium / dark shading corresponds to <40, [40-55], >55% of episodes in the season). Hatched (grey) cells identify aerosol types with less than 20% of occurrence (no episodes) in the given season.

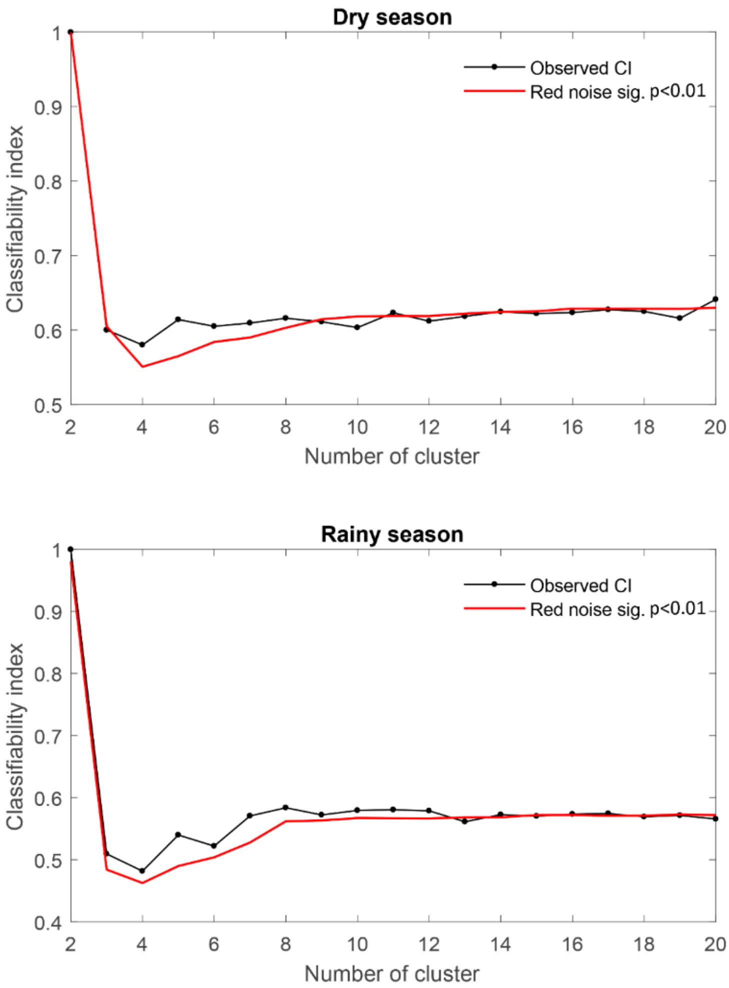

Figure A1. Classifiability index CI distribution against the number of clusters. The black line shows the observed CI. The red solid line is the one-sided $p<0.01$ significance level from 100 red-noise simulations.